Technical Report No. 43

SACLANT ASW
RESEARCH CENTRE

SOUND ATTENUATION BETWEEN 200 AND 10,000CPS MEASURED ALONG SINGLE PATHS

by

C.C. LEROY

1 SEPTEMBER 1965

NATO
VIALE SAN BARTOLOMEO, 92
LA SPEZIA, ITALY

TECHNICAL REPORT NO. 43

SACLANT ASW RESEARCH CENTRE
Viale San Bartolomeo 92
La Spezia, Italy

SOUND ATTENUATION BETWEEN 200 AND 10,000 CPS MEASURED ALONG SINGLE PATHS

By

C. C. Leroy

1 September 1965

APPROVED FOR DISTRIBUTION

W. C. Wineland

W. C. WINELAND
Deputy Director

TABLE OF CONTENTS

SOUND ATTENUATION BETWEEN 200 AND 10, 000 cps MEASURED ALONG SINGLE PATHS

By

C. C. Leroy

ABSTRACT

In the deep Mediterranean basins, the water is perfectly isothermal below 400 m, and the deep refracted ray gives clear signals up to 40 km, with a spreading loss free from any frequency-dependent effect. Exploiting this unique opportunity, a frequency analysis has been performed between 200 and 10, 000 cps on the waveforms of acoustic signals from explosive sources, which had travelled along this path. Statistically, the change of spectrum with range is due only to absorption and internal spectral arrangements of the shock-wave energy. Seven independent acoustic runs were analyzed which led to similar results. The average gives a detailed accurate curve of relative attenuation between 500 and 8000 cps. Among the possibilities of placing this curve in absolute scale, the one giving a best fit to a variation in f^2 at low frequencies is found (a) to agree when extrapolated with values already published below 200 cps, (b) to be well-represented by $a = Af^2 + Bf_o f^2/(f_o^2 + f^2)$, where Af^2 is the classical absorption and where f_o = 1.7 kc. Some discussion follows about the interpretation of the results.

INTRODUCTION

The attenuation of low frequency sound (below 10 kc) in sea water is very small and its measurement requires the study of long ranges of propagation in order to obtain a sufficient accuracy. This is why measurements at low frequencies are usually made by a frequency analysis of the total acoustic energy received along a sound channel from an explosive sound source. This technique assumes that the variation of the energy spectrum with range is due only to attenuation. This hypothesis is better verified at very long ranges when the wave guide effect is well established. As a first consequence, the measurements become more uncertain as the frequency increases toward the higher frequencies, because the received levels are too low. Even then, the structure of the sound channel and the reflecting properties of the boundary (sea surface and sea floor) may alter the quality of the wave guide. This is especially true above 0.5 kc, as the bottom losses begin to vary appreciably with frequency for a given incident angle of the sound.

In principle, measurements via single paths present still greater difficulties: as the possible path length is limited, the excess of propagation loss to be measured becomes very small at low frequencies. In addition, propagation via single paths is greatly affected by the structure of the velocity profile: i.e., slight irregularities of the profile give rise to anomalous frequency-dependent spreading losses with the higher frequencies following roughly the ray theory, while the lower frequencies no longer conform. The spreading loss irregularities depend too much on the frequency and reach values that are too high when compared with the small attenuation effects investigated.

The result of this situation is that attenuation in sea water is not well known below 10 kc and especially in the medium range between 0.5 and 8 kc. Sheehy and Halley data[1], published eight years ago, were long the only information available,

but these were concerned with frequencies between 20 and 200 cps. Above 200 cps, extrapolation was assumed on the basis of a variation in $f^{1.5}$ up to 10 kc; the exponent 1.5 was obtained from a best fit of the low frequency data point. However, this extrapolation gave higher values than the classical absorption values established from the relaxation of magnesium solfate.

Three years ago, while analyzing sound channel measurements, the SACLANT ASW Research Centre (SACLANTCEN) found attenuation values between 0.5 and 5 kc that were greater than those suggested by Sheehy and Halley. Although the SACLANTCEN measurements lacked sufficient accuracy to be conclusive, they did indicate a need for further research. A first examination of the available recorded data indicated that attenuation can be accurately measured in the Mediterranean along single paths in the frequency band of interest. Obviously, advantage had to be taken of this.

As pointed out earlier, irregularities in the velocity profile complicate attenuation measurements along single paths; however, the Mediterranean has a unique temperature structure which allows such measurements with accuracy. Throughout the entirety of this sea, all important variations of temperature occur between the surface and 100 m of depth; between 100 m and 400 m the variations never exceed $\pm 1^{\circ}C$, and below 400 m the water is practically isothermal at $13^{\circ}C$ down to the bottom irregardless of depth. Under these conditions, large masses of homogeneous water can be found with thicknesses up to 2500 m and horizontal dimensions of more than 50 km. Deep refracted rays propagate very regularly in such waters; due to the pressure effect, the rays are constantly bent upward by a quasi-constant velocity gradient. Spreading losses between source and receiver are not affected by any frequency dependent factor in the frequency range of the desired data. The mean variation of the frequency spectrum of an explosive sound pulse with range can be due only to attenuation or, possibly, to finite amplitude effects.

The SACLANTCEN study began in April 1963. A restricted area was selected for which magnetic tape recordings, suitable for analysis, were already available from several acoustic runs. This paper describes the measurements, the analysis methods, and the results of the first study.

In the meantime, various authors[2-5] have emphasized the need for measurements in this frequency band; some of these authors point out the possibility of a new interpretation of the Sheehy-Halley results, as well as the danger of slightly different results of attenuation according to whether explosions or CW pulses are used. All these points have been considered; it was felt most desirable to obtain the maximum accuracy in the shape of the attenuation vs frequency curve — precision has been the primary care in this analysis, and the results give the limits of confidence of the measurements. Discussions of the possible interference of finite amplitude effects are also included. The analysis shows that a relaxation process of about 1.7 kc is most probably responsible for the excess of attenuation found in these measurements.

New data on attenuation[6-9] have been published more recently which concern the results of sound channel studies; some of these confirm the general trend reported here.

I. EXPERIMENTAL CONDITIONS AND TRIAL DESCRIPTIONS

The results in this paper are from the analysis of various experiments which were not performed to measure attenuation. A small area was selected which had a variety of suitable data recorded on magnetic tape for different locations, times of the year, and recording equipment. The locations and dates of the trials used in this analysis are shown on Fig. 1*. Only the useful section of each run is indicated; this was limited to 40 km for Runs A through F and to 12 km for Run G, which corresponds to a different geometry.

The bathymetric structure and related velocity profile varied between the various experiments; Fig. 2 shows the limiting cases and some examples. It can be seen in the figure that all major variations occur at depths less than 100 m. Below 100 m (in almost all cases) the water is practically isothermal, except for an increase of about $0.5^{\circ}C$ around 200 - 300 m; below 500 m the temperature is isothermal at $13.0^{\circ}C \pm 0.1^{\circ}$.

Salinity follows roughly the same pattern and is practically constant at 38.45‰ at all depths greater than 300 m. The slight increase in temperature around 300 m is typical of the Western Mediterranean. Although this increase is very small, it is of considerable importance to this work, because it causes propagation instability in acoustic paths of interest. For simplicity, this layer between 200 and 400 m will be called the "unstable" zone in this paper. The minimum sound velocity was between 60 and 150 m and, in all cases, the acoustic paths below 500 m were fractions of circles corresponding to propagation in a constant velocity gradient medium.

The SACLANTCEN Research Vessel (receiving ship) drifted freely during all trials; for runs A through F, the principal recording devices on board this ship

*All figures are at the end of the text.

were a hydrophone (suspended to 100 m), a variable gain amplifier, and a magnetic tape recorder. The overall recorded frequency band varied between the lower limit of 70 to 150 cps and the upper limit of 5 to 12 kc. The hydrophones, cut off frequencies, and tape recorders were varied for the different trials but remained absolutely the same for any one, except in Runs E and F when different hydrophones were used for short and long ranges. For these two runs, although the data were corrected to account for the difference in hydrophone frequency response, there was a degradation in the accuracy of the method, and the analysis was limited to 5 kc.

The sound sources used in Runs A through F were 180 gm TNT charges in a cylindrical metal case, set to detonate hydrostatically at 100 m. The variance in explosion depths was only 5 m; on the source peak level, it was less than 1 dB. The firing ship proceeded at constant speed along predetermined tracks and dropped the explosives periodically. This ship also carried a hydrophone and paper-recording device which marked the exact time that the sound was received from each explosion. The difference between this time and the time of the last acoustic arrival (SOFAR ray) at the receiving ship was used to compute the distance between the source and receiver. The shortest ranges recorded were between 200 and 400 m, the longest useful ranges about 38 km; the range accuracy for all measurements was estimated to be about 80 m.

The following discussion concerns the acoustic paths of interest for attenuation measurements, as taken with the geometry described above. (See Fig. 3).

At ranges up to 1 km, the acoustic path of interest was the one direct path (not surface reflected) which corresponded to an almost straight line and whose propagation was most regular. Beyond 1 km, new direct paths became evident and, as the range increased, a sound channel was progressively built-up. From

about 1-2 to 15-20 km, the section of the deep refracted ray which traveled in the unstable zone was predominate, and the angle of this ray with the horizontal while in the zone was very small; consequently, propagation was irregular and presented multipaths and frequency dependent effects. From about 20 to 40 km, the sequence of arrivals definitely began with a clear deep refracted ray, which for the most part had travelled in the constant gradient deep water and had crossed the unstable zone with an angle steep enough to eliminate any possibility of irregular spreading loss. As a consequence, the change in spectrum with range could be attributed to attenuation only for the direct arrival at short ranges and for the deep refracted arrival at ranges of more than about 20 km.

Two further limitations restricted the cases of possible analysis.

(1) Finite amplitude effects that occur in a high-peak pressure shock wave result in a change of waveform with range. These effects must be negligible when compared to those caused by attenuation; consequently, measurements at very short ranges would be eliminated. However, with charges as small as 180 gm TNT, the finite amplitude effects were considered negligible at 200 m, which was the minimum range of this analysis. This point will be discussed later.

(2) The arrivals of interest must be sufficiently separated in time from the other arrivals to enable analysis. At short ranges (over 800 m), the surface reflected arrival often arrived very close to the direct and at long ranges the same occurred with the bottom reflected and the deep refracted arrivals. Consequently, a number of events were eliminated from the analysis. In the medium ranges, the time separation between the deep refracted arrival and the subsequent arrival was generally greater than 8 ms and thus allowed a frequency analysis on the shockwave down to 200 - 300 cps. On the contrary,

the arrival of the bubble pulse acoustic signal, corresponding to propagation by the deep refracted ray, was generally mixed with the other shockwave arrivals. Only in rare cases was it possible to isolate it for a few milliseconds by high-pass filtering, but no systematic analysis was possible. Therefore, the study will concern only shockwave analysis for the first six runs.

Figure 4 demonstrates the geometry of Run G: two hydrophones in a vertical line were suspended from the receiving ship to near the bottom. The uppermost hydrophone, 2300 m deep and 150 m above the bottom, was used to record data for analysis. The second hydrophone was mounted 50 m below the first. The difference in the times of arrivals at the two hydrophones was used to compute the angles of arrival of the acoustic rays, and the horizontal ranges and ray path lengths between the source and the recording hydrophone.

The sound sources for this run were 500 gm TNT charges set to explode at 400 m. As on the other runs, they were launched by the firing ship while opening in ranges. Radar ranges were used as a check against those computed by ray angle determinations.

With this geometry, the deep refracted ray arrived first, followed by the bottom reflected ray, and then by the surface reflected ray, etc. For the deep refracted ray, there was no frequency dependent effect or spreading loss for the total range of possible distances. However, at very short ranges, the sound arrived almost vertically at the hydrophone. The omnidirectionality of the hydrophone was not perfect up to such angles and the sound spectrum was altered. Above 3 kc the analysis, which will be described later, had to be limited to rays with a horizontal angle of less than 45^{o}. The usable path lengths were limited between 2-5 and 13 km for the shock wave arrivals. At the lower frequencies, this upper limit went down to 10 km for the bubble path arrivals, as the bottom reflected ray followed too closely. In all cases, the small interval of suitable ranges limited the analysis to frequencies above 800 cps.

II. MEASUREMENTS OF THE WAVE FORM SPECTRA

The first step in the analysis was the preparation of a complete set of oscillograms, such as shown in (b) of Fig. 5, for all explosions of all runs. These were used to select the events suitable for analysis.

Distorted signals (e.g., the 14 km oscillogram) were eliminated along with events with insufficient time separation, low signal to noise ratio, etc. Detailed oscillograms of all waveforms to be analysed were then made from the master tapes, enlarged photographically, and sampled manually. A Fourier analysis was then made on an electronic computer with the series of sample amplitudes.

In all cases for any given run, the playback instrumentation remained rigorously the same for the analysis of all waveforms; however, the equipment's frequency band varied from one case to another. First, the amplitude of a signal had to be back at the zero line within reasonable limits before the next arrival. This was accomplished by selecting a proper low cut-off frequency; however, a compromise was usually necessary, because the short and long range events allowed a lower cut-off than those of medium range. Second, the highest frequency possible varied from one run to another, due to the noise level or simply to instrumentation. Consequently, the total frequency range of the analysis was divided into one, two, or three slightly overlapping bands, according to the case. This method reduced the total number of samples that had to be read to cover the entire frequency band of interest. Again, a compromise was needed on each run to avoid the preparation of an exagerated number of oscillograms. Some examples of oscillograms with the sampling frequencies are shown in (c) of Fig. 5. In some cases it was possible, at least in the oscillatory decay phase, to operate a smoothing of the waveform, and thus improve the signal to noise ratio at high frequencies, or to eliminate weak interfering signals. An example is shown with the 42 km oscillogram in Fig. 5(c).

The oscillograms were enlarged to about 5 x 15 in., and the sample amplitudes were read separately by two operators with exceptional care in the leading sections. The average readings were punched on paper tape for computer processing. To make the effects of spectrum folding negligible, an adequately high sampling frequency was always chosen. In principle, this frequency was more than twice the mean of the 3 dB and the 40 dB down frequencies of the filter. In many cases, the duration of the samples portion was artificially increased by adding zeros to the sample amplitude series. This did not add information at the lower frequency end, but it did increase the number of definition points in the spectrum. The computer programme gave the Fourier components in dB vs 1 mm on the oscillogram.

III. COMPUTATION OF SOUND ATTENUATION FROM THE SPECTRUM VARIATION

In this first analysis, it will be assumed that the change of spectrum with range is caused only by attenuation, and that finite amplitude effects do not exist at 200 m (the shortest range in the trials). The validity of this assumption will be examined in the next section and a second analysis will be made.

Given the frequency spectrum of all the oscillograms; various methods, which mainly depend on the following alternatives, are possible to establish an attenuation vs frequency curve.

1.(a) Absolute attenuation values may be computed independently at various frequencies.

(b) Differential attenuation values between frequencies may be computed, and the results may be used later to obtain an absolute curve.

2.(a) Measurements may be made independently for each acoustic run and the results averaged later.

(a) All spectra from the various runs may be considered as part of a single family; the range is the only variable, and average attenuation values may be computed directly.

Methods 1(b) - 2(a) were adopted for this analysis with the objective to obtain the best possible accuracy in the shape of the attenuation vs frequency curve. The justification of the methods and comparisons with alternate methods will be presented in the description of the analysis technique. To facilitate discussion, the following terminology will be used: (all frequencies are in kilocyles).

$S(f)$ Average acoustic spectrum level of the source in dB (re 1 dyne/cm^2 at 1 m distance) at frequency f.

X_i Range in kilometres from the source for explosion i.

$a(f)$ Attenuation coefficient at frequency f in dB/km.

$N_i(f)$ Noise level at frequency f in the recording of explosion i.

$\ell(f, X_i)$ Spectrum level in dB re 1 mm at frequency f as given by the computer for explosion i at range X_i.

δ_i Ray angle with horizontal at the source of the deep refracted ray for explosion i.

As we are in a constant velocity gradient medium, the average spreading loss between 1 m and range X_i(km) is:

$$\text{spreading loss in dB} = 20 \log (X_i / \cos \delta_i) + 60$$

This formula is derived directly from ray equations and, since the ray curvature radii are sufficiently large, it is valid for the entire frequency range used.

The path length L_i may be approximated by the range X_i. It is easy to verify that $1 < L_i/X_i < 1.005$ at all ranges; consequently, the relative computation error of the differential attenuation coefficients caused by this simplification will be less than 0.5% and perfectly negligible.

Both the source level and the spreading loss may fluctuate slightly in a random manner around their average values. Let $\sigma_i(f)$ and $\epsilon_i(f)$ be the value of these fluctuations at frequency f for explosion i. Under these conditions

$$S(f) + \sigma_i(f) - 60 - 20 \log (X_i/\cos \delta_i) - \epsilon_i(f) - a(f) \times X_i + N_i(f) =$$

$$= \ell(f, X_i) + K(f) + G_i$$

where $K(f) + G_i$ accounts for the entire record playback sensitivity from the acoustic signal in the sea at the receiver to the analysis oscillograms. It is divided into 2 parts:

1. K(f) - takes into account the frequency response of the entire equipment, which remained unchanged during each run and its analysis.

2. G_i - represents the overall gain and sensitivity settings, which were independent of frequency but varied from one explosion to another. (In particular, G_i includes the term $-20 \log T_i$, where T_i is the duration of the signal used in the Fourier analysis.)

In addition to the real fluctuation already written into the equation, there are the following instrumental or calibration errors on each of the measured quantities S, X, ℓ , and K:

δS which varies with f only and comes from calibration errors.

δX which varies with i only and has been seen to be of the order of 0.08 km.

$\delta \ell$ which varies with both f and i independently and arises from instrumental errors and analysis inaccuracies.

δK which varies with f and may, at first approximation, be regarded as independent of i.

δG_i which varies with i only.

Equation (1) can then be applied, replacing S by $S + \delta S$ (where S is the result of the measurements and $S + \delta S$ is the exact unknown value), etc.

Description of the Method. The amplitudes of the Fourier components, given in dB by the computer, were plotted versus frequency for each oscillogram, and a smooth spectrum was drawn across the data points. On all runs the levels $\ell(f, X_i)$ were read off these spectra at the following pre-determined frequencies f_p:

0.2, 0.3, 0.4, 0.5, 0.6, 0.7, 0.8,

1, 1.2, 1.5, 2, 2.5, 3, 4, 5, 6, 7, 8, kc

For each run, a number of reference frequencies f_o (usually two) were chosen from the above list in each frequency band used for oscillograms. The differences of spectrum levels $\Delta\ell_{p,o,i} = \ell(f_p, X_i) - \ell(f_o, X_i)$ between the frequencies of the above list and the reference frequencies were then calculated. If we apply Eq. (1) for one explosion i and two frequencies, and if we also introduce the errors δS, δX, etc., we can write

$$\Delta\ell_{p,o,i} = \left[H(f_p) - H(f_o)\right] + \left[\delta H(f_p) - \delta H(f_o)\right] - \left[a(f_p) - a(f_o)\right] \cdot \left[X_i + \delta X_i\right] + \left[\eta_i(f_p) - \eta_i(f_o)\right] \tag{2}$$

where the term

$$H(f) = S(f) - K(f) \tag{3}$$

is a calibration constant, independent of the explosion, known with the error $\delta H = \delta S - \delta K$ and where

$$\eta_i(f) = \sigma_i(f) - \epsilon_i(f) + N_i(f) - \delta\ell_i(f) \tag{4}$$

is a fluctuation error, dependent on the explosion.

From Eq. (2), it is straight forward that (when plotted versus range X_i in a linear scale) the measured difference $-\Delta \ell_{p,o,i}$ should give points scattered around a straight line, whose slope is the differential attenuation coefficient $\Delta a_{p,o,} = a(f_p) - a(f_o)$. This procedure was applied systematically and illustrations are given in Fig. 6.

The three spectra in part (a) of Fig. 6 correspond to the real analysis results in the frequency band 240-3700 cps of three explosions from Run D. One of the reference frequencies was 1.5 kc, and the example of the readings of spectrum level differences between this frequency and two others is given in part (a) of the figure. These differences are also plotted on the $-\Delta \ell$ vs X diagram in part (b) together with similar readings from other explosions of this run. The linear variation is evident. Another example is given in part (c) for the same frequencies and another run where, although the number of points is much reduced, the linear tendency is still clearly apparent. The straight lines in parts (b) and (c) are the result of linear regression calculations that were performed by an electronic computer from the coordinates of the data points. These computations assume no error in range measurements; i.e., they neglect δX_i with the justification that $\delta X_i < 0.1$ km and that the value X_i extends up to 40 km.

The computer gave the slope $b = \Delta a_{p,o}$ of the regression line with its standard error SE. The linear regression technique was applied for all data and the analysis provided a series of differential values along with the corresponding standard errors. Special attention was given to minimize the influence of the spreading of points around the regression line which comes from the fluctuation term $\eta_i(f_p) - \eta_i(f_o)$. The term $\delta \ell_i(f)$ represents the only instrumental errors which contribute to the spreading of points; these errors are mainly due to the analysis technique of the oscillograms (readings of the sample values,

estimations of the smooth spectrum to be drawn from the computer results, etc.) To minimize fluctuations, very great care had to be given to the analysis and, in addition, the quality of the data in the regression computation had to be considered. A discussion of this consideration follows.

As a constant frequency band (resulting from a compromise) was used to make all oscillograms for any one run, it was known in advance where the spectra would eventually be altered: toward the low frequencies if some extrapolation of wave forms were necessary; toward the high frequencies if the noise levels were too high. Thus, the unreliable fractions of the spectra were omitted from the readings. Furthermore, it very often occurred that a spectrum was more regular or better defined for some frequencies than for others, or that the quality of the oscillograms was obviously better for some events. These factors were introduced by using the best data points in the regression analysis twice. Comparisons with the results from the unweighted points proved that the standard error on the regression line slope was reduced appreciably. The points used twice are shown in part (b) of Fig. 6 by open circles.

It can now be seen that it is inadvisable to use all data points in all runs in a single regression analysis. The term $\left[\delta H(f_p) - \delta H(f_o)\right]$ in Eq. (2) is an invariant during one run, and it does nothing other than to alter the ordinate at zero abscissa of the regression line. Had all points from all runs been put together $\left[\delta H(f_o) - \delta H(f_o)\right]$ would have been a new fluctuating quantity because $\delta K(f)$ depends on the run. This new fluctuation is the calibration precision; as its order of magnitude is 1 to 2 dB, the variance of the regression line slopes would be seriously increased. On the contrary, the accuracy will be much higher for an analysis where measurements are done independently for each run and the results are averaged afterwards. In addition, we wanted to see if there were appreciable differences of attenuation values from one location and period of time to another. This will be discussed later.

Similar considerations on the magnitude of the fluctuation show that absolute measurements at each frequency would lead to less accurate results. Equation (1), with the error terms δS, δX, etc., gives:

$$\ell(f, X_i) + 20 \log \frac{X_i}{\cos \theta_i} + G_i = \left[H(f) + \delta H(f) - 60\right] - a(f) \left[X_i + \delta X_i\right] + \left[\eta_i(f) - \delta G_i - \delta\left(20 \log \frac{X_i}{\cos \theta_i}\right)\right] \quad (5)$$

The fluctuation term can be approximated as $\cos \theta_i \simeq 1$, by:

$$\psi_i(f) = \eta_i(f) - \delta G_i - 8.6 \frac{\delta X_i}{X_i}$$

The fluctuation was previously $\left[\eta_i(f_p) - \eta_i(f_o),\right]$ and its variance was found to be of the order of 1 to 1.5 dB so that the variance of $\eta_i(f)$ can be expected to be roughly 1 dB. The additional fluctuations in $\psi_i(f)$ are independent of f. The term δG_i is of the order of 0.2 to 0.5 dB only, but as $\delta X_i \simeq 80$ m, the last term will reach 3.5 dB for a range of 200 m.

It is straight forward from part (b) of Fig. 6 that the short range data points have a paramount importance on the regression line slope, because of the lack of data between 2 and 20 km. Since the short range points are scarce (three at 300 m in Run D, one at 300 m and one at 2 km in Run C, etc.) an error as high as 3 dB on their ordinate would completely ruin the analysis. Although the regression line slopes would be altered in the same direction for all frequencies, the magnitude of their alteration would depend on the frequency. Similarly, the standard error given by the regression analysis would increase considerably, especially at low frequencies where the slope is small. The final results of such an analysis would be erratic and the confidence interval too broad to provide a valuable knowledge of attenuation as a function of the frequency.

In contrast, the analysis that was performed gave a whole series of differential attenuation coefficients, each with a smaller confidence interval. The results of this technique, as applied to 6 runs, will be presented in the next section.

Various solutions were possible to derive a single curve of absolute attenuation versus frequency from this set of data. For example, the averages of differential attenuation values could have been made and an absolute curve derived from these values. However, in order to control the universality of the results on the classical representation a(f) in logarithmic scale, it was considered more valuable to derive absolute values from each run, although the two methods would have given almost identical final results.

Considering the data from one run only, it appears that the entire absolute attenuation curve might be derived from one absolute measurement at one frequency. For such a measurement, there is an optimum accuracy frequency zone that results from a compromise between sufficiently high values of a(f) and sufficiently low values of the fluctuation $\psi_i(f)$ which, due to background and analysis noise, increases with frequency. In the present case, the greater relative accuracy for absolute measurement was in the region of 2 - 6 kc. It is easy to demonstrate that such a method is not entirely satisfactory. Figure 7 illustrates the deformation of the attenuation vs frequency curve (in the usual logarithmic presentation) when the absolute value of 5 kc is changed by 2.5, 5, and 10%, and all differential values are held absolutely constant. The "exact curve" on the figure is an anticipation of the one which will be proposed later. The figure shows that an error of +5% at 5 kc would result in an error of + 700% at 500 cps and in a curve with a completely different shape. To have reasonable values at 300 cps, an accuracy of at least 2% is required, which does not take into account the error on the differential values themselves. Such accuracy is hard to achieve and was not possible on these trials. An absolute measurement

at a lower frequency would be less accurate and would result in the same uncertainty on the final curve. To summarize, the differential values and some absolute measurements may be used only to build a whole family of possible curves that are known individually with good accuracy and limited by the extreme curves of the absolute measurements. On the contrary, absolute measurements at each frequency would give one curve that is known with much less accuracy and situated within the same extreme curves, but which does not necessarily belong to the family.

In order to make a choice between possible curves, it was assumed, in accordance with the idea expressed by Schulkin[2], that at very low frequencies attenuation varies as the square of the frequency. Consequently, an adjustment to such a variation was made by successive approximation in two steps for each run.

The first step was to choose 700 cps (in some cases 500 cps) as the basic reference frequency. The differential attenuation coefficients with respect to this frequency were plotted on a diagram with a quadratic frequency scale for all frequencies up to 1 kc. To account for known standard errors of the differential coefficients in making the best fit to a straight line, it was assumed that the ordinates of all points, including the reference frequency were affected by smaller or greater "fluctuations". These fluctuations were defined as being such that the sum of the square of the fluctuations at frequencies f and 700 cps was equal to the variance on the differential attenuation coefficient between these two frequencies. It was first checked, by an examination of the differential errors between 600, 700, 800, and 1000 cps and the adjacent reference frequency (usually 1500 cps), to see that the fluctuation at 700 cps was not greater than that at the neighboring frequencies, i.e., that the errors on the differential values referred to 700 cps did not come from an abnormal behaviour of the spectrum at precisely 700 cps — it was proved that this did not happen in any case. The fluctuation at 700 cps

was then evaluated from the table of differential standard errors (usually it was taken as the smallest differential error divided by $\sqrt{2}$). The other fluctuations were computed by applying the principle of quadratic additions mentioned above. The data points and their fluctuations were plotted on the diagram, and an estimate of the best-fit straight line was drawn together with the possible extreme lines. The intersection of these lines with the zero frequency axis gave a first estimate of the absolute zero on the attenuation scale with the possible errors. All absolute values were read from this zero at each frequency, and the error at each frequency was computed by taking into account the error on the zero adjustment and the previously computed fluctuations. From this adjustment at the low frequency end and from the tables of differential coefficients, the absolute values of attenuation coefficients were then calculated by progressing toward the higher frequencies.

The standard errors on these absolute values were also calculated. Six of the seven runs were analysed independently by this method and an average of the results was computed. In view of the differences of accuracy obtained in the different runs, statistics were applied for this averaging as follows. A weighted mean of the absolute attenuation coefficients of all runs was computed at each frequency, and the values with the smallest standard errors were given the most weight. The standard error on this mean was computed at the same time. The resulting data points, when plotted in the usual logarithmic scale were found to be aligned along a smooth curve. It was easy to establish that an equation could be written with the form

$$a(f) = Af^2 + \frac{Bf_r f^2}{f_r^2 + f^2} \qquad (6)$$

to represent the curve.

However, the first analysis proved that, in the frequency band used to calculate the absolute scale (0.3 - 1 kc), a variation of attenuation such as $a(f) \sim kf^{1.78}$ would represent Eq.(6) better than a variation in f^2: the frequencies involved were not low enough for the equation to be approximated by $a(f) = B/f_r \cdot f^2$.

The entire procedure as previously described was repeated in a second step, replacing the original adjustment to a law in f^2 by an adjustment to a law in $f^{1.78}$. Examples of such adjustments are shown in Fig. 8, where two cases are given: one with a good accuracy on adjustment, and one with a large uncertainty. By applying this method, new zeros on the attenuation scale were found for each run and a new series of attenuation coefficients were computed. As before, a weighted mean was calculated, which gave the final data points and their standard errors. It was then possible to adjust the final curve, defined by Eq.(6) to these points.

IV. EXPERIMENTAL RESULTS

The results of the analysis of shock wave arrivals of Runs A through F are discussed in this Section. The values of Run G were not accurate enough to be included (the ranges were too limited); these results and the bubble pulse analysis will be found in Section V. For ease in comparison, some results have been grouped into tables which will be constantly referenced in the following discussions.

Runs A and B were performed in sequence and with the same equipment. In these runs only one close range explosion was found suitable for analysis. The corresponding spectrum data have been used for the regression analyses of both runs, which is entirely justified since close range data cannot be expected to vary with location and since the equipment remained rigorously the same for both runs. The analysis could be performed only on a limited number of explosions, corresponding to the following ranges in kilometers:

Run A: 0.5, 23.2, 27.3, 29.3, 31.5, 33.2, 39.5

Run B: (0.5 from Run A), 26.1, 27.2, 29.6, 31.8, 32.0, 36.0

Two series of spectra (I and II) were measured for these runs. Series I was obtained from the analysis of the wide band waveforms (180-8000 cps), in which case the oscillograms of the complete waveforms were duplicated by an oscillogram of the first peak only, made with an enlarged time scale. This permitted an accurate measurement of the sample levels all along the waveform. The resulting spectra were considered up to 5 kc only, and the differences of spectrum level were read, using the reference frequencies of 700 and 1500 cps. Series II was measured from filtered oscillograms (frequency bands 2.5-20 kc), and 5 kc was the reference frequency for the measurements of level differences.

The number of spectrum level differences used in the regression analyses for these runs can be found in Table I.* The data points have been weighted 1 or 2, according to the degree of certainty of the spectrum and the clarity of the oscillogram. The resulting differential attenuation coefficients are given in Table II.

Run C was made with almost the same equipment as A and B; the technique used to obtain spectrum level differences was rigorously identical. The explosions of interest correspond to the following ranges in kilometers:

0.3, 2.1, 16.2, 19.4, 21.0, 22.0, 28.5, 30.0, 31.5.

Again, the number of explosions is moderate, but the range coverage is better assured than previously. For the first series of oscillograms, no waveform or spectrum was found that was definitely better than another; consequently, all data points have been given the same weight in the regression analysis. For the second oscillogram series (7.5 - 10 kc), weights were assigned as in Runs A & B. The spreading in differences of spectrum levels may be considered as typical; this is demonstrated in Table III. Figure 6, which illustrates the regression analysis, gives some of these data plotted against range. As for the other runs, the number of computation points used for each differential attenuation coefficient can be found in Table I and the results in Table II.

Run D was the most complete in the analysis; the linear density of explosions along the run was higher, and a total of 29 events were usable in the measurements. The corresponding ranges in kilometers were:

0.3, 0.3, 0.3, 20.0, 20.0, 20.0, 21.2, 22.1, 23.8, 24.3, 25.0, 26.0,

27.0, 28.7, 29.4, 30.0, 30.5, 31.0, 31.5, 32.5, 33.0, 34.5, 35.8,

36.2, 37.4, 38.0, 38.7, 39.5, 40.4.

*All Tables are presented at the end of the text, immediately after the figures.

The analysis of this run was the most elaborate: three series of oscillograms were made for frequency bands 280 - 1050, 240 - 3700, and 2400 - 9600 cps. In the lowest band, the spectrum level differences were read with respect to 500 and 800 cps, and 900 cps was added to the list of predetermined frequencies. As all oscillograms and spectra were of good quality, the assignment of different weights to the points in the regression analysis was not considered justifiable, although some weighted analyses were performed for comparison.

For reading the differences of spectrum level for the second and third series of oscillograms, 0.8 and 1.5 kc and 3 and 5 kc were used respectively as the reference frequencies. Since the noise level had altered some recordings more than others in the higher frequencies, weights equal to 1 or 2 were applied to the data in all cases in the regression analysis. The results are given in the tables.

The last two runs, E and F, were performed with the same equipment. An exception for these runs, the recordings were limited to 6.5 kc by instrumentation. The waveform spectra were measured, as in Runs A and B, from wide-band oscillograms with additional enlargements of the initial pressure peak. The reference frequencies were 0.7 and 1.5 kc, and the regression analyses were made with weighted data. The ranges in kilometers were:

Run E: 0.2, 0.4, 0.6, 15.8, 18.3, 20.8, 23.3, 25.7, 28.2, 30.7, 33.0, 35.4, 37.2

Run F: (0.2, 0.4, 0.6 - all from Run E), 18.8, 20.0, 23.8, 26.3, 28.7, 31.3, 33.6

As in Runs A and B, the short range data for Run E were used in both analyses. However, since these short range explosions were recorded on different hydrophones, a proper correction had to be applied to account for the different

frequency responses. This correction was less accurate with increasing frequency, and weights of 1, 2/3, and 1/3 were given to these points according to the case and the whole analysis was limited to 5 kc. The other data points were given weights of 1 or 2 as in the previous runs.

Table I indicates all the linear regressions that have been performed and the number of independent data points (i.e., the number of differences of spectrum levels without consideration of their weight in the analysis), which was used in each case. The indication is made by an indexed letter when the data were used with all the same weights. The term "Ref" on each line marks the reference frequency which was used for the regression analyses indicated in the same line. A total of 140 linear regressions were made, a number of which were performed mainly to provide a check on values already computed (particularly in the overlapping frequency bands) or to verify that the spectrum level at the basic frequency for the adjustment in $f^{1.78}$ did not fluctuate more than at the adjacent frequencies.

An examination of the differential attenuation coefficients in Table II shows that there is a good agreement above 800 cps between the values obtained from the various runs. The existing differences are compatible with the values of standard errors. Run D gave the smallest standard errors, while Runs C, E, and F are generally the least accurate, although the number of suitable explosions was greater than in Runs A and B. The slight variations that can be observed in the differential values between two adjacent frequencies, computed from two different sets of differential values, result from the differences in number of points and in the weights used in each linear regression. This difference results from the fact that, for all the explosions concerned in a linear regression, the measurements did not generally have the same accuracy (or could not always be performed) at the two or more reference frequencies f_o used in the analysis. These points justify the use of several reference frequencies. It was very often found that the

errors on the difference of attenuation coefficients between a high frequency and a low reference frequency were smaller when this difference was computed with the aid of an intermediate reference frequency: more and/or better data points could be used in the linear regression concerning the medium frequencies.

The adjustment to a variation in f^2, then in $f^{1.78}$, was made independently on each run as explained in the last section. This adjustment could be made accurately for Run D, where the analysis in the low frequency band (280 - 1050 cps) provided good data. A basic frequency of 500 cps was chosen for the adjustment in Run D; 700 cps was used for the other five runs. The variation of attenuation as $f^{1.78}$ was still evident for Run A, although it led to smaller than average attenuations. The adjustment was less accurate or less realistic for the other runs, especially Run F, which presented a marked minimum attenuation at 500 cps. However, the errors in adjustment were not found to depend on the legitimacy of the adjustment to a law in $f^{1.78}$ precisely. Two examples are given on Fig. 8: (1) a precise adjustment (corresponding to Run D); (2) an inaccurate adjustment (corresponding to Run C).

The best fits in $f^{1.78}$ for the different runs may be expressed by the following values of attenuation at 700 cps with their estimated errors of adjustment. (The original value of Run D at 500 cps is also given and marked with an asterisk).

Run	A	B	C	E	F	D	D*
Attenuation ($dB/km \times 10^{-3}$)	27	70	68	32	41	40.7	22.5
Adjustment Error ($dB/km \times 10^{-3}$)	5	18	12	10	12	9.3	3.0

*500 cps

Absolute values of attenuation with their standard errors were computed by continuous progression from low to high frequencies for all runs from the previous values of adjustment and Table II. However, the fact that some values could be obtained by different approaches was also considered. For example, in Runs A, B, and C the absolute value at 5 kc was obtained from the value at 3 kc, plus an average of the differential values between 3 and 5 kc that was obtained from the analysis of the first and second series of oscillograms. These results are plotted on Fig. 9 which, for sake of clarity, does not indicate standard errors. It can be seen that there is a very good agreement in the general trend of the variation with frequency; the spreading of points is consistent with the calculated errors.

Figure 10 presents the results of averaging the values. The points indicate the mean weighted values, and the vertical segments crossing these points represent the limits of confidence given by plus or minus twice the standard errors. The points are perfectly aligned along a smooth curve from which it was easy to establish the representative equation

$$a(f) = Af^2 + \frac{Bf_r f^2}{f_r^2 + f^2}$$

In this instance, however, it was not considered practical to compute A and B by a best fit method performed by an electronic computer, as this would have led to unrealistically complex coefficients. An approach by trial and error, using only simple coefficients with two significant figures for f_r, led to

$$a(f) = 0.006f^2 + \frac{0.155f_r f^2}{f_r^2 + f^2} \qquad (7)$$

where a(f) is in decibels per kilometer, f is in kilocycles, and f_r = 1.7 kc.

The curve corresponding to this equation is drawn on Fig. 10 . It is first pointed out that the term 0.006 f^2 is suitable in this frequency domain to represent the pure absorption of magnesium sulfate relaxation. The coefficient agrees with the classical values corresponding to the constant temperature of 13°C encountered in the experiments. The remaining factor accounts for a relaxation process at 1.7 kc and the possible existence of such a low frequency relaxation was suggested by Schulkin[2]. It is most remarkable also that the extrapolation of data at the lower frequencies by Eq.(7) agrees with Sheehy and Halley[1], who made completely different experiments in different waters. The Sheehy and Halley data are given for comparison on the figure, both for the original adjustment to a variation in $f^{1.5}$ and for the adjustment to an f^2 law, which Schulkin proposed later.

It can also be seen from Fig. 10 that the values of attenuation lie within the limits of the absolute measurements performed on 6 runs at 4 kc. These measurements were made by the method described in Section III and with Eq.(5). This time, it did not appear justifiable to use different weights for the data points in the linear regression, because an oscillogram or spectrum that is better defined than another does not necessarily correspond to an explosion for which the sound level, record/play-back gain, and range are also better known. In addition, the close range points were deleted from the analysis. (Their use, with the necessary introduction in the regression analysis of the possible error $-8..6\ \delta X_i/X_i$, was found to lead to a greater inaccuracy in the result !). The

results of each run were as follows:

Run	A	B	C	D	E	F
Attenuation ($dB/km \times 10^{-3}$)	350	174	120	361	150	288
Adjustment Error ($dB/km \times 10^{-3}$)	161	94	113	65	139	43

The weighted mean of these results leads to a(4 kc) = 0.269 dB/km with a standard error of 0.031 dB/km. The limits have been drawn on the figure, as previously, on the basis of twice the standard error. A similar computation was performed for 3 kc, which led to an attenuation of 0.219 dB/km with a standard error of 0.042 dB/km. The inaccuracy of these measurements is evident; however, it is seen that the values thus computed are higher than the classical absorption would predict.

V. SECOND INTERPRETATION OF THE DATA

In the last section, the resolution of attenuation values from the waveform spectrum variation was based on the assumption that only attenuation was involved. The entire analysis was performed on shockwave arrivals, and it was assumed that the finite amplitude effects had already disappeared.

The question of the range at which finite amplitude effects exist is the subject of some controversy. According to various authors or theories, the effect would cease after a certain range, or tend to an asymptotic law that differs from classical acoustics. It was considered here, for 180 g TNT charges exploded at 100 m depths, that the effect would not exist at 200 m from the source. The peak pressure at this range is 6.3×10^5 dyne/cm^2, while the hydrostatic pressure is 1.1×10^7 dyne/cm^2; i.e., 17 times higher. Thus, it can be reasoned that the theory of small perturbation would begin to be valid. This logic is, of course, over-simplified, because the original sound transmission was a shock wave which is more complex than a simple very high pressure pulse. However, if an analysis on shock wave gives important errors, the preceding indicates that the same errors would not occur from a similar analysis on bubble pulse arrivals, because the acoustic signals from bubble pulses do not have the same dispersive behaviour. To take advantage of this, bubble pulse arrivals have been analysed whenever possible. As already stated, it was extremely difficult to isolate the corresponding waveforms in time, so the complete analysis described in Section III was impossible. However, in Run C, it was possible to compute some differential attenuation values in the frequency range 1.5 to 4 kc by the same regression analysis techniques. The results are found in Table IV.

It is immediately apparent that these differential values are inaccurate, and that they are even greater than those obtained from shock wave analysis. In all cases the values are out of proportion with those given by the classical absorption $0.006f^2$.

Run G gave a better opportunity to compare measurements from shock waves and bubble pulses. Although this run was not suitable for complete analysis, due to poor accuracy at low frequencies and to the impossibility of a best fit to a variation in f^2, its geometry made it possible to measure differential attenuation coefficients between 0.8 and 4 kc from both the shock wave and the bubble pulse arrivals analyses. The results are given in Table V.

It may be seen from the table that the values agree among themselves and with those from other runs. Again, the values are higher than those given by absorption. The conclusion from these last data is that the excess of attenuation given in Eq. (6) by $0.155\, f_r f^2 / (f_r^2 + f^2)$ cannot all be attributed to the fact that explosives were used as a sound source.

Although it was considered improbable that finite amplitude effects still existed at the ranges of these trials, a new analysis was carried out with differential values $\Delta \ell_{p,o,i} = \ell(f_p, X_i) - \ell(f_o, X_i)$ from a number of acoustic runs. In this analysis, the extreme case of the existence of finite amplitude at all ranges was adopted. The differences of spectrum levels were corrected to subtract the effect of finite amplitude. The corrections that were used were derived from the most classical theory,[10] based on the following hypothesis:

1. Originally, the full band shock wave has the shape of an infinitely abrupt rise, followed by an exponential decay.

2. The peak pressure of this pulse varies with range in an infinite homogeneous, non-absorbing medium as $p(x) = k \left(W^{1/3}/X\right)^{\alpha}$, where W is the weight of the explosive.

3. The time constant of the exponential decay varies with range as $\Theta = k' W^{\beta/3} X^{1-\beta}$.

Under these assumptions, it is easy to establish that the power spectrum at range X is given by

$$s(\omega) = \frac{2p\,\theta^2}{\pi(1+\omega^2\,\theta^2)} \tag{8}$$

This frequency spectrum varies continuously with some energy being transferred from the higher to the lower frequencies. The alteration of the spectrum, due to finite amplitude effects only, can then be calculated by applying Eq. (7) to the case of 180 g TNT with the "Arons values" for k, k', α, and β. The difference of spectrum levels (in decibels) at range X between frequencies f_o and f_p is represented by

$$S(f_p, X) - S(f_o, X) = 10 \log \frac{1 + 0.145\, X^{0.44} f_o^2}{1 + 0.145\, X^{0.44} f_p^2} \tag{9}$$

These quantities were calculated with $f_o = 0.7$ kc for various frequencies f_p and ranges X up to 42 km (the maximum range in the trial). The difference $\left[S(f_p, X) - S(f_o, X)\right] - \left[S(f_p, X_o) - S(f, X_o)\right]$ was computed with $X_o = 42$ km and plotted on a diagram as a function of range for various frequencies.

Figure 11 shows the resulting curves for the relative changes of the spectrum, as the range decreases from 42 km to 200 m, which could be attributed to finite amplitude effects. It can be seen that there are minor changes in the spectrum above 2 kc for the entire domain of ranges considered and that the variations are always small above 0.5 kc between 15 and 40 km.

Readings off the figure were used to correct the values of $\Delta\ell_{p,o,i}$ at various frequencies in a number of runs, and regression analyses were made with these corrected data. Figure 12 gives typical examples. The new regression lines

of $-\Delta \ell$ on X are indicated together with the previous ones from the uncorrected data. It is quite apparent that the previously observed linear variation is now considerably affected, mainly due to the ordinate change of the short range points. This tends to prove that no finite amplitude effects exist at 200 m from the source. However, the results of this new regression analysis were exploited, and Table VI gives some new values of differential attenuation coefficients, with their standard errors, computed from the data of Runs A, C, D, and E after correction.

It can be seen that, after correction, the low frequency values are much more inaccurate than before and lead to unrealistic results. No best fit to a variation in f^2 can be attempted and, in general, there is a minimum attenuation frequency. If the value zero is taken for the attenuation at the minimum attenuation frequency, absolute values can be deduced in the entire frequency range of measurements. These values, which represent the minimum that attenuation can reach, have been plotted in Fig. 13. A smooth curve A has been drawn from these points; this curve defines the approximate domain (the hatched area below the curve) in which attenuation values are unrealistic. It is therefore concluded that, if finite amplitude effects (as defined by classical theory and available data for the parameters) exist at all ranges encountered in these measurements, there is still an excess of attenuation for which these effects cannot account. Under these conditions, sound attenuation by sea water would probably be represented by a curve between the limits of Curve A and Curve B, which was previously proposed by Eq. (7). Curve C gives an idea of the possibility. This curve, which is given only for illustration and does not correspond to measurements, matches the Sheehy and Halley data (with the f^2 adjustment) and still corresponds to a relaxation process with a frequency of 1.7 kc.

CONCLUSION

Due to its isothermal deep water, the Mediterranean provides an excellent opportunity to use single paths to obtain attenuation values by studying the variation with range of the waveform from an explosive sound source. This technique presents various advantages: measurements may be made within the frequency range where data are needed; these measurements are free of various assumptions and inaccuracies encountered when propagation along a sound channel is used to determine attenuation. The acoustic path used in this study is the deep refracted path along which energy propagates most regularly up to sufficient ranges. If the source and receiver are deeper than 400 m in the Mediterranean, there is no spreading loss anomaly in the frequency band of interest that is due to temperature irregularities, and the curvature of the ray is too small to introduce distortion. These ideal conditions were effectively realized in the sea trials of this study. The use of the 100 m source and receiver introduced distortions at ranges between 2 and 20 km only, and the corresponding arrivals were deleted from the analysis. Compared with the sound channel measuring technique, the depth of the water reached by the ray is the only parameter which can influence sound attenuation and does not stay constant with range in the use of the single path. However, this effect is not critical. In particular, and since the water is isothermal in this case, one of the possible causes of attenuation variation is thus eliminated, and the single parameter, variation with frequency, can be studied with greater accuracy. As a matter of fact, it is the last variation that one must know to understand the phenomenon, and it has been shown that the differential method is more appropriate to achieve this purpose. Precise values of differential attenuation coefficients can be obtained; from these, absolute attenuation can be computed to one constant in the whole frequency range of interest. This constant may be determined independently from an absolute measurement at one frequency. With the available data however, it was found that this measurement

was not accurate enough, and more accurate absolute values were computed by an appropriate assumption. This assumption leads to the concept of a low frequency relaxation mechanism. It can be shown that such a mechanism is the most likely to occur, and it is remarkable that a first adjustment to a variation at f^2 at the lowest frequencies in the analysis of the present data led to a whole curve of attenuation which corresponds to a relaxation process. The other possible mechanisms are less likely to be responsible for the excess of attenuation reported here. Scattering may reasonably be eliminated; as propagation is studied here along single paths with omnidirectional sources and receivers. Furthermore, scattering could not account for Eq. (7).

Waveform distortion caused by finite amplitude effects is another possible cause of apparent attenuation. The single path technique requires the use of short signals to resolve the time of the proper arrivals. In this respect, explosive sound sources are best, and they provide data in the whole frequency range where they are needed. However, explosive sources present nonlinear effects near the source whose results could be misinterpreted for attenuation. This did not seem to be the case in these measurements. If finite amplitude effects can be assumed to alter the waveforms at all ranges, the analysis has demonstrated that: (a) the expected linearity of variation of spectrum level differences with range is distroyed; (b) the calculated values of attenuation are more incoherent and inaccurate, and (c) there still exists an excess of attenuation above 1.5 kc which is almost as important as before.

The analysis which led to these results was performed with the classical theory and parameters and, in view of the measurements reported here, it is not unlikely that some of the data on finite amplitude effects should be revised. As a matter of fact, these effects and the attenuation of sound both contribute to alter the waveform and the spectrum of an explosive sound source. One way to separate

these effects clearly is to make a continuous and accurate study of the waveforms received at all ranges from very short to very long. Other authors have suggested such measurements.[12] A complete frequency analysis is required, and more information is gained by a simultaneous study of the amplitude and the phase variation. On the contrary, the study of only the peak level variation of explosive signals might cause inaccurate results, since the peak pressure is also altered by attenuation in a way which seems difficult to predict and which could be neglected in the analysis.

Based on the assumption that finite amplitude effects do not account for the excess attenuation reported here, and since the measurements fit perfectly to an interpretation by a relaxation method, it appears that Eq. (7) can be proposed to represent attenuation in sea water. Schulkin[2] proposed eddy viscosity as a possible acoustic absorption mechanism, and referred to a frequency of relaxation which is lower than the one found here, although the order of magnitude remains in the same frequency range. If eddy viscosity were really responsible, it could occur that the size of the eddies would depend (among others) on the orientation with respect to the vertical and on the depth. In this case, the values reported here would require a slight correction, since the rays were traveling at different depths at different ranges; however, it seems that this correction would be a magnitude of secondary order. In particular, no evidence has been found of a systematic departure from a linear variation in the study of the differences of spectrum levels between fixed frequencies as a function of range.

It must still be established whether or not this relaxation phenomenon depends appreciably on the type of sea. In this respect, the Mediterranean appears to offer more homogeneous water than other seas; this could lead to different results. Unfortunately, as has been shown, similar measurements are more difficult in other seas. However, attenuation values obtained elsewhere and by different

methods (particularly Schulkin[2] and Thorp[6]) are almost the same at the lower frequencies as those found here; this tends to favor, at first approximation, the universality of the phenomenon and the values of the proposed attenuation.

ACKNOWLEDGEMENTS

The author wishes to thank Mr. N. Stenseng of the University of Oslo, Norway, and Mr. J. Gerrebout of the SACLANT ASW Research Centre, La Spezia, Italy for their help in data reduction.

REFERENCES

1. M. J. Sheehy and R. R. Halley, J. Acoust. Soc. Am., No. 29, p. 464, 1957.

2. M. Schulkin, J. Acoust. Soc. Am., No. 35, p. 253, 1963.

3. H. W. Marsh, J. Acoust. Soc. Am., No. 35, p. 1837, 1963.

4. C. B. Brown and S. J. Raff, J. Acoust. Soc. Am., No. 35, p. 20007, 1964.

5. H. W. Marsh, "Distortion of Propagating Underwater Signals," paper presented at the NATO Advanced Study Institute of Grenoble (France), 14-26 Sep. 1964.

6. W. H. Thorp, "Attenuation Studies," paper presented at the Navy Symposium: Underwater Acoust., 20th, 13-15 Nov. 1962 (Unpublished).

7. T. J. Urick, J. Acoust. Soc. Am., No. 35, p. 1413, 1963.

8. J. D. Macpherson and N. O. Fothergill, "Acoustic Propagation in the Nova Scotian Sound Channel," paper presented at the 67th Meeting of the Acoust. Soc. Am., 6-9 May 1964 (Unpublished).

9. P. G. Hansen, "Measurement of Attenuation of 5 to 8 kc Sound in Small Samples of Sea Water," paper presented at the 68th Meeting of the Acoust. Soc. Am., 21-24 Oct. 1964 (Unpublished).

10. R. H. Cole, "Underwater Explosions," Princeton University Press, Princeton, New Jersey, 1948.

11. A. B. Arons, J. Acoust. Soc. Am., No. 26, p. 343, 1954.

12. H. Christian, W. H. Marsh, etc.

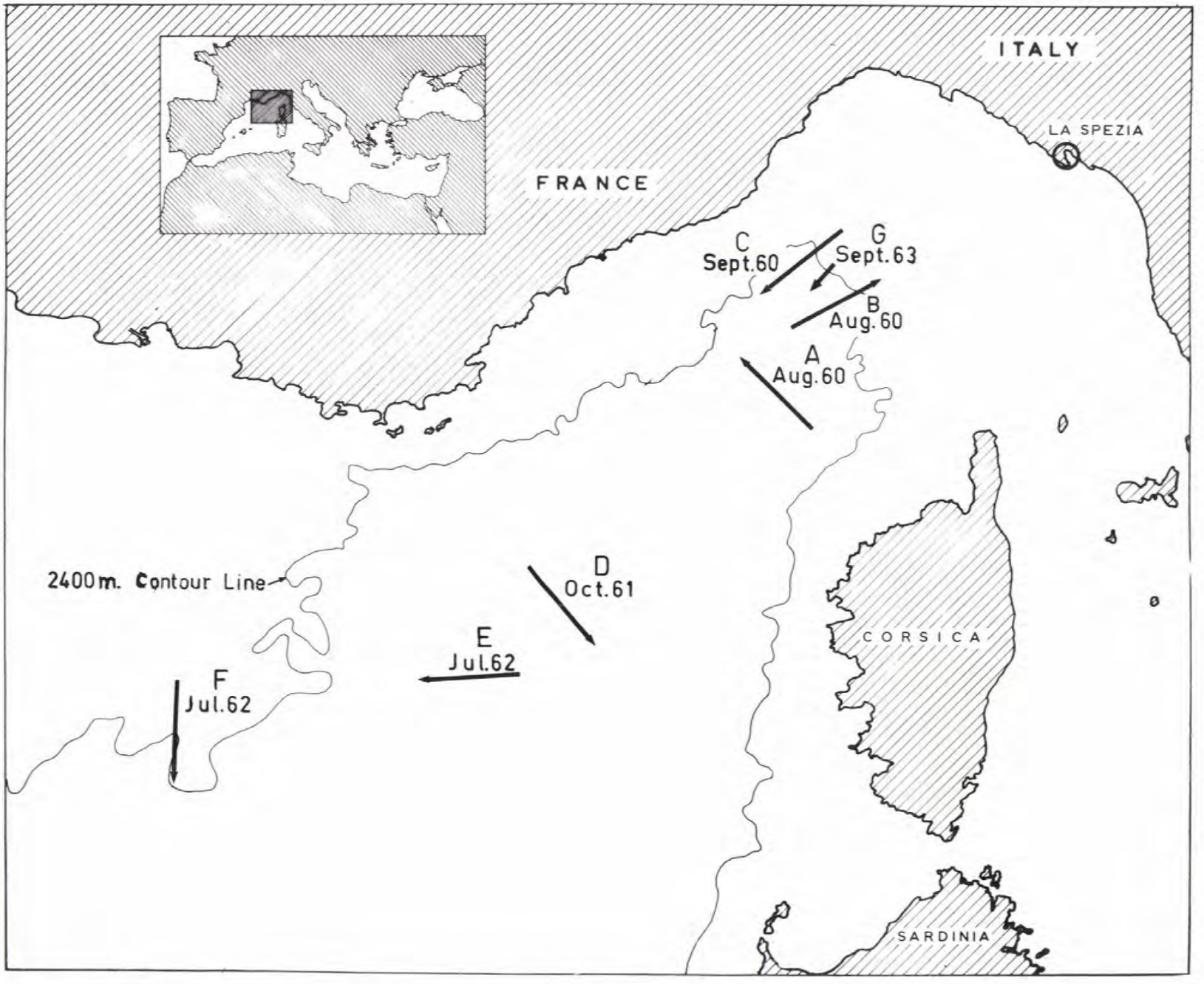

Fig. 1 - LOCATIONS AND DATES OF TRIALS.

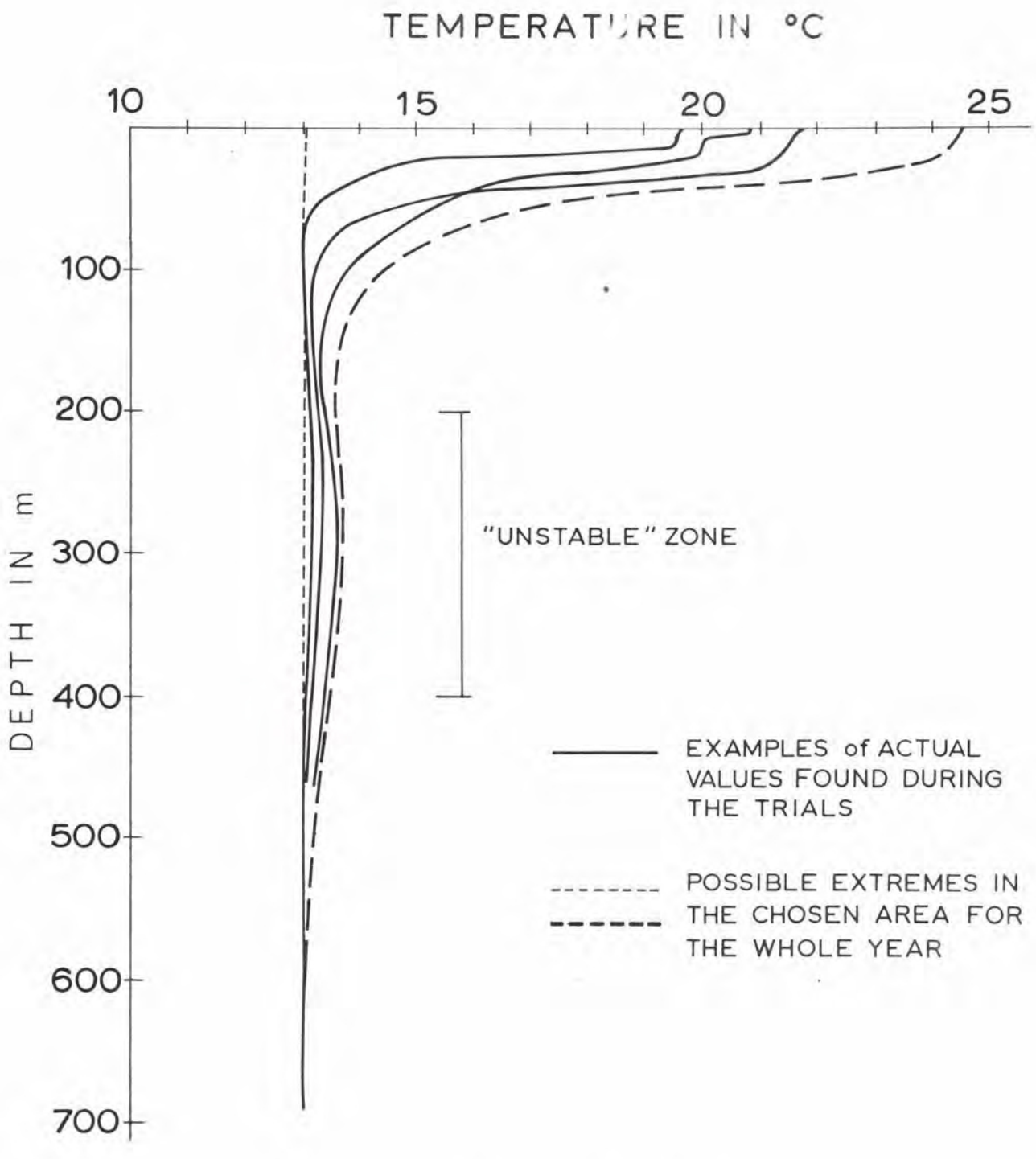

Fig. 2 - TEMPERATURE PROFILES IN THE TRIAL AREA.

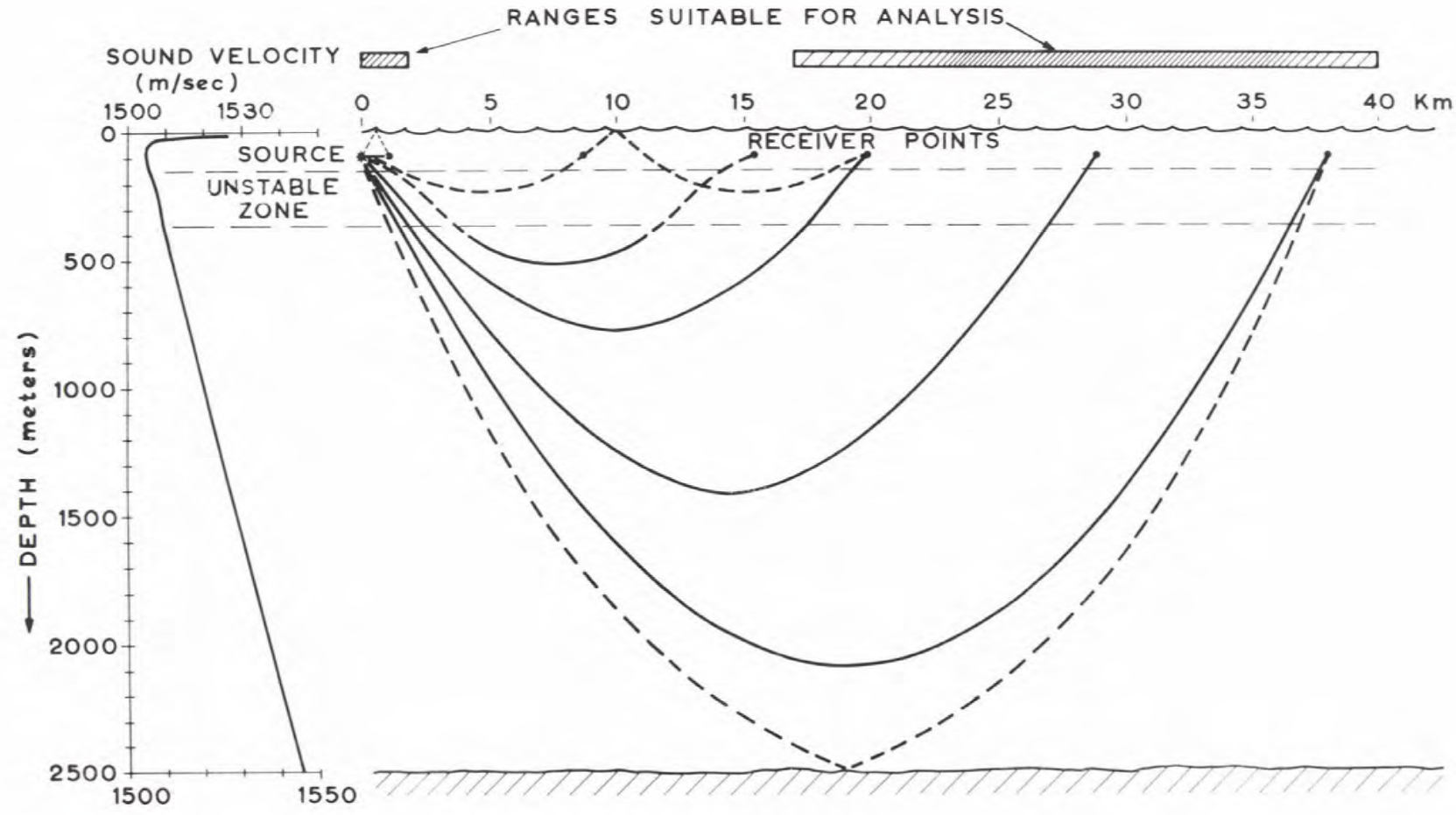

Fig. 3 - VARIATION OF RAYS WITH RANGE DURING RUNS A THROUGH F.

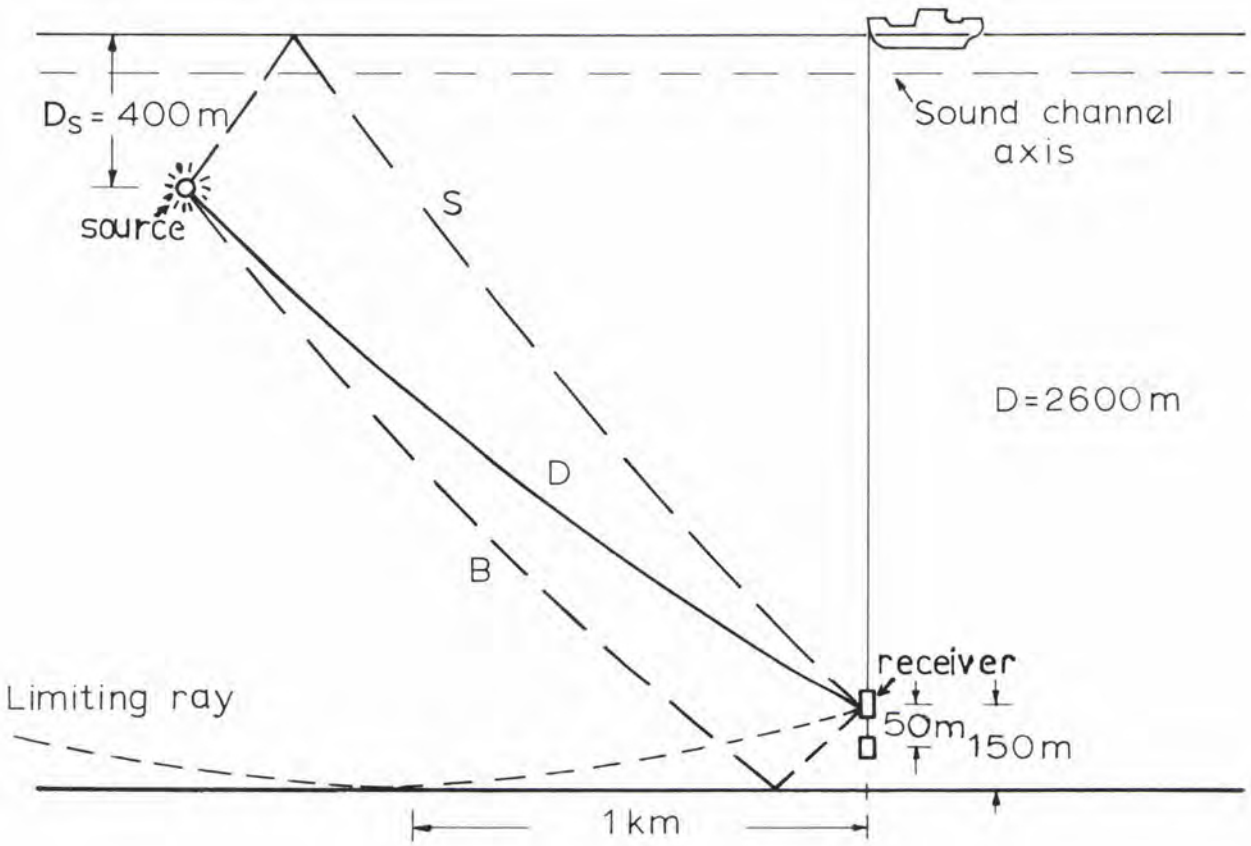

Fig. 4 - RAY DIAGRAM FOR RUN G.

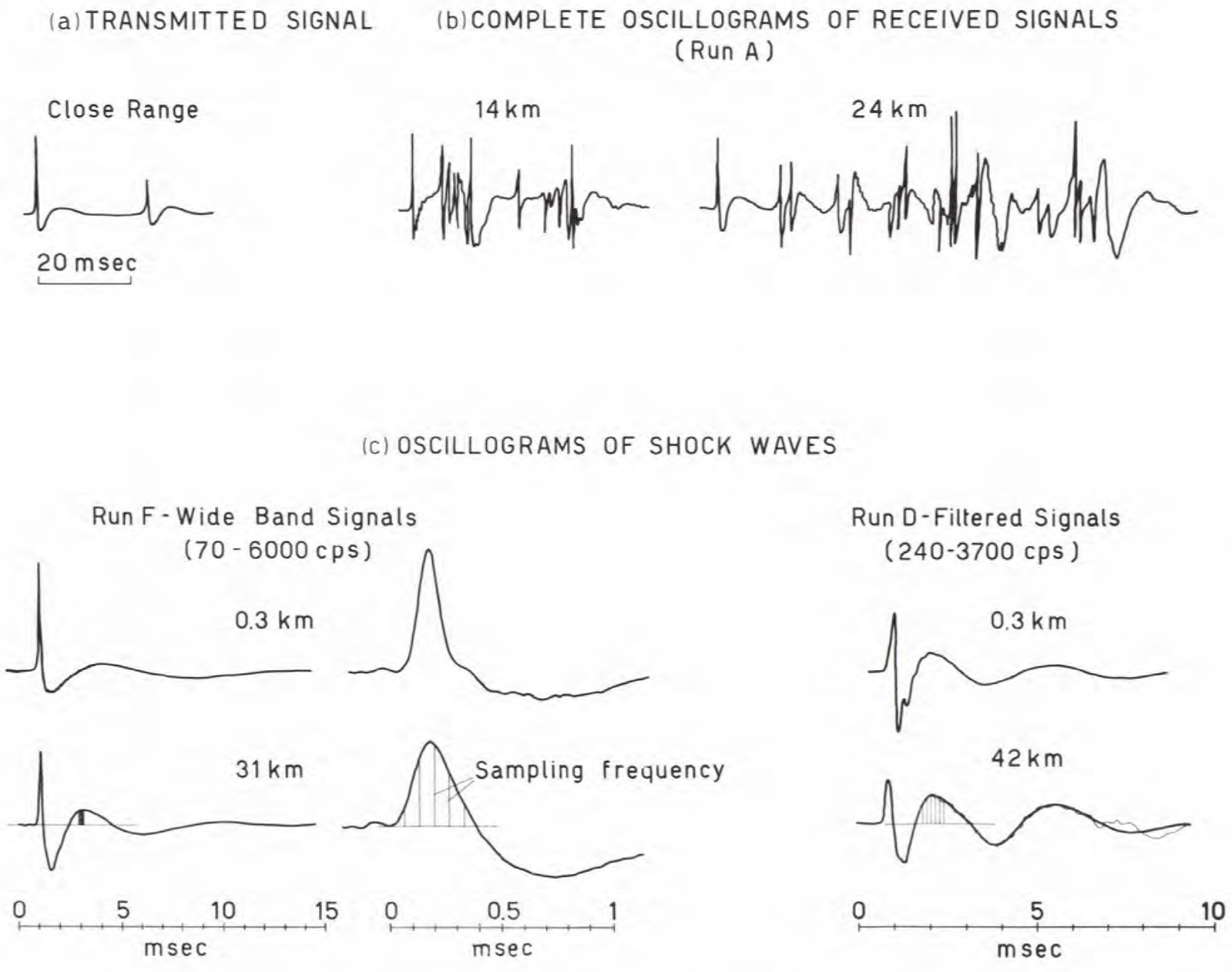

Fig. 5 - EXAMPLES OF OSCILLOGRAMS OF THE RECEIVED ACOUSTIC SIGNALS.

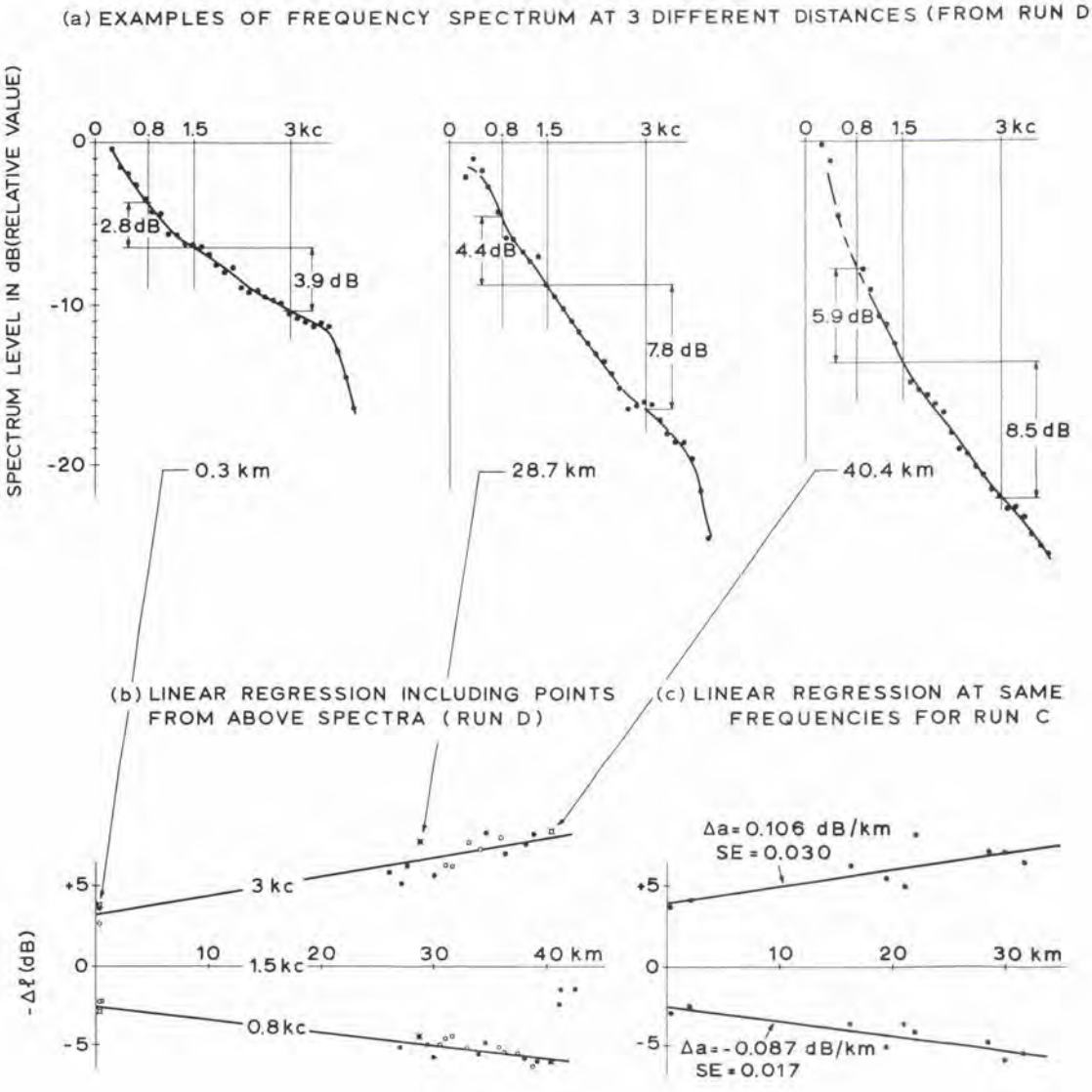

Fig. 6 - METHOD USED TO COMPUTE DIFFERENTIAL ATTENUATION COEFFICIENTS FROM FREQUENCY SPECTRA.

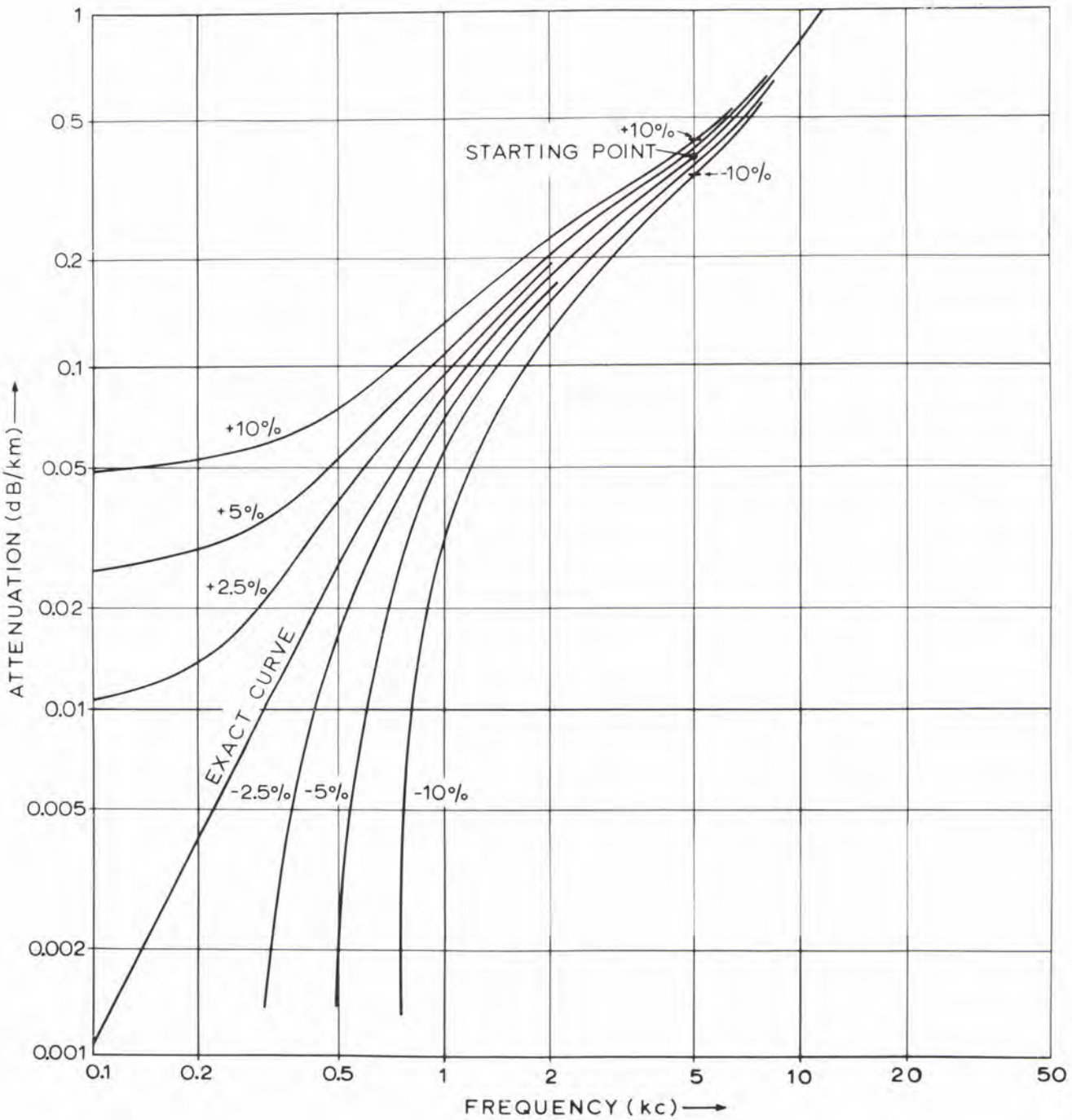

Fig. 7 - DEVIATION FROM THE EXACT ATTENUATION CURVE FOR DIFFERENT ERRORS IN THE ABSOLUTE VALUE AT 5 kc.

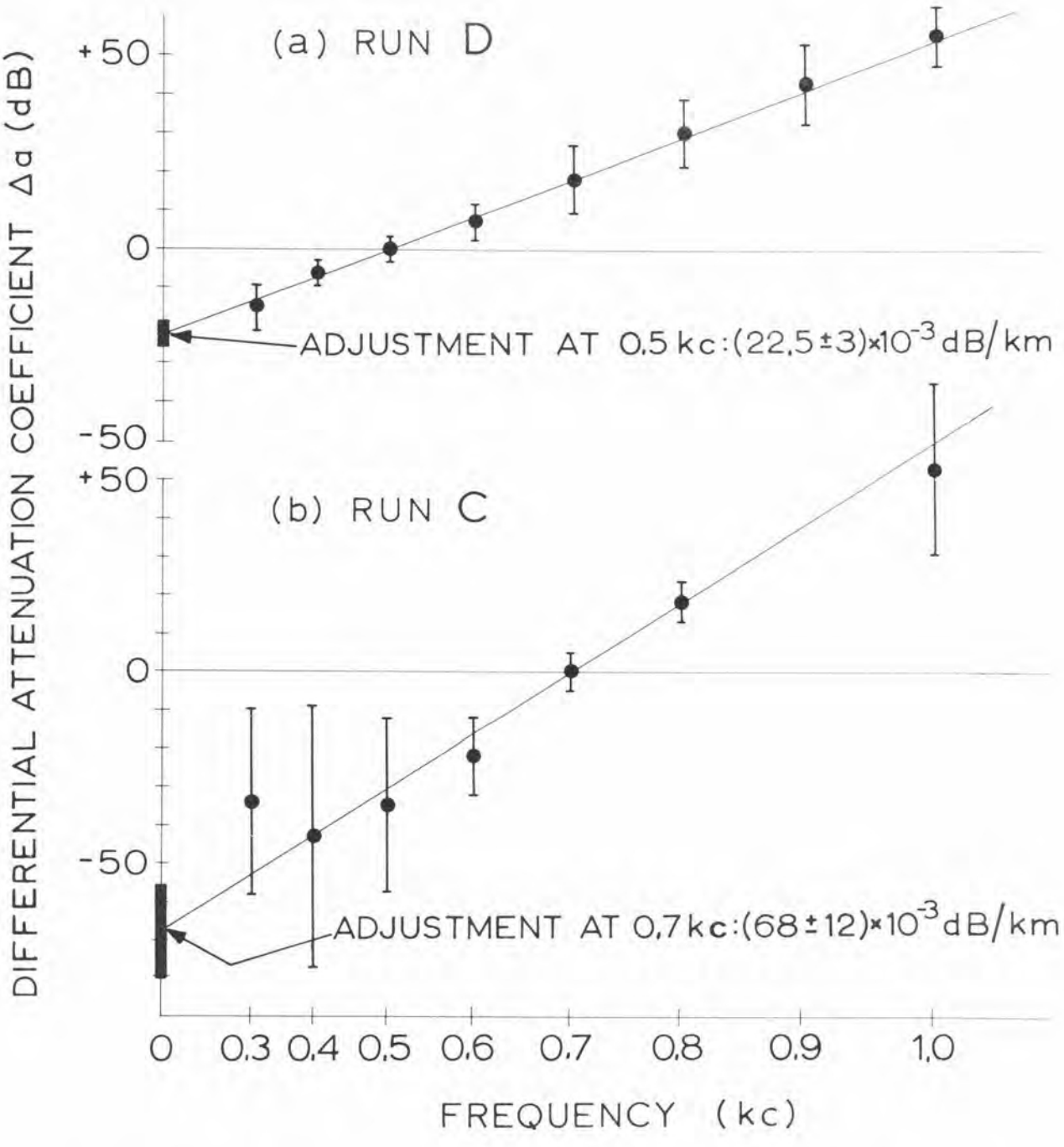

Fig. 8 - EXAMPLES OF ADJUSTMENT OF ATTENUATION VALUES TO A LOW FREQUENCY VARIATION IN $f^{1.78}$

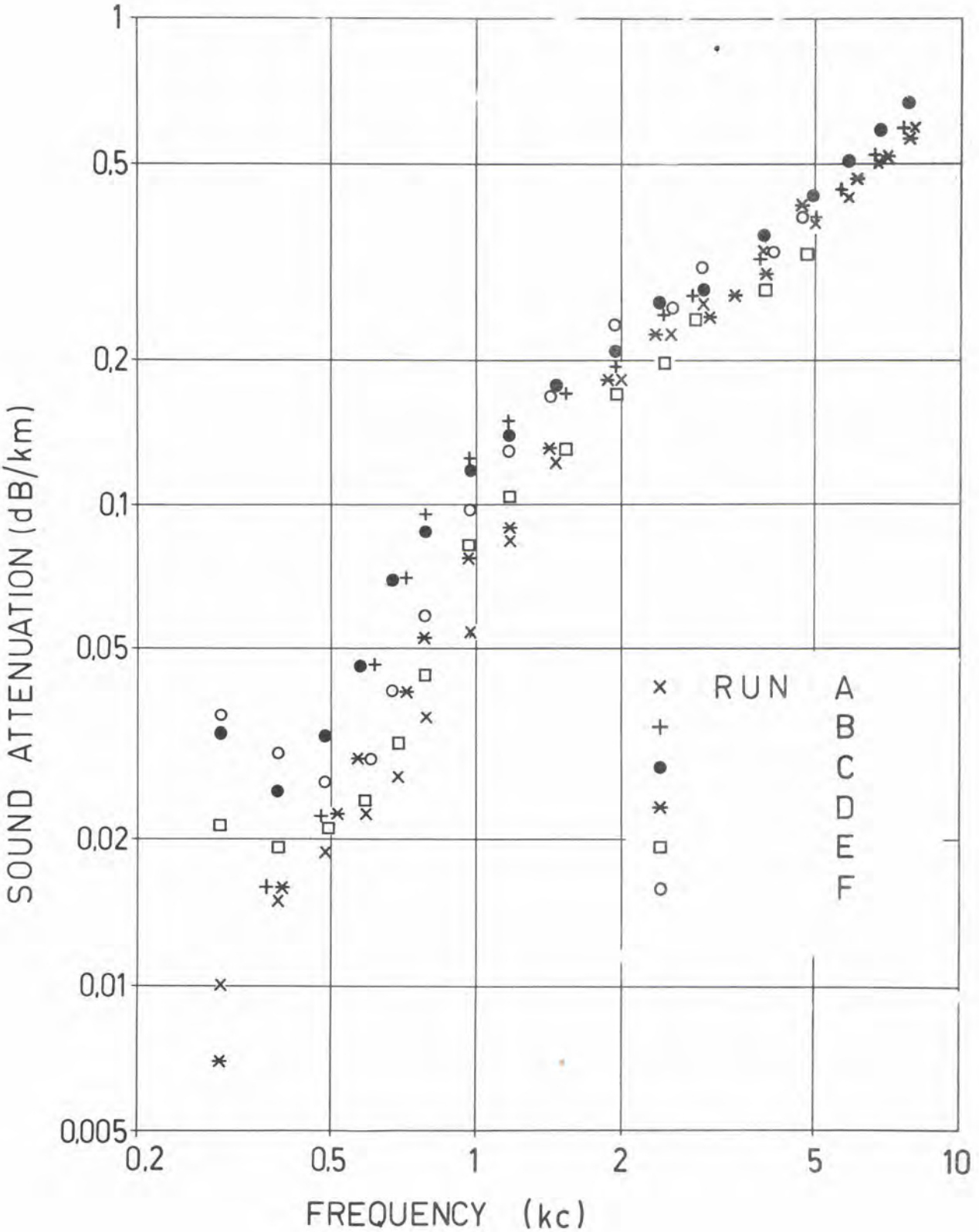

Fig. 9 - SOUND ATTENUATION vs FREQUENCY — INDIVIDUAL RESULTS OF SIX RUNS.

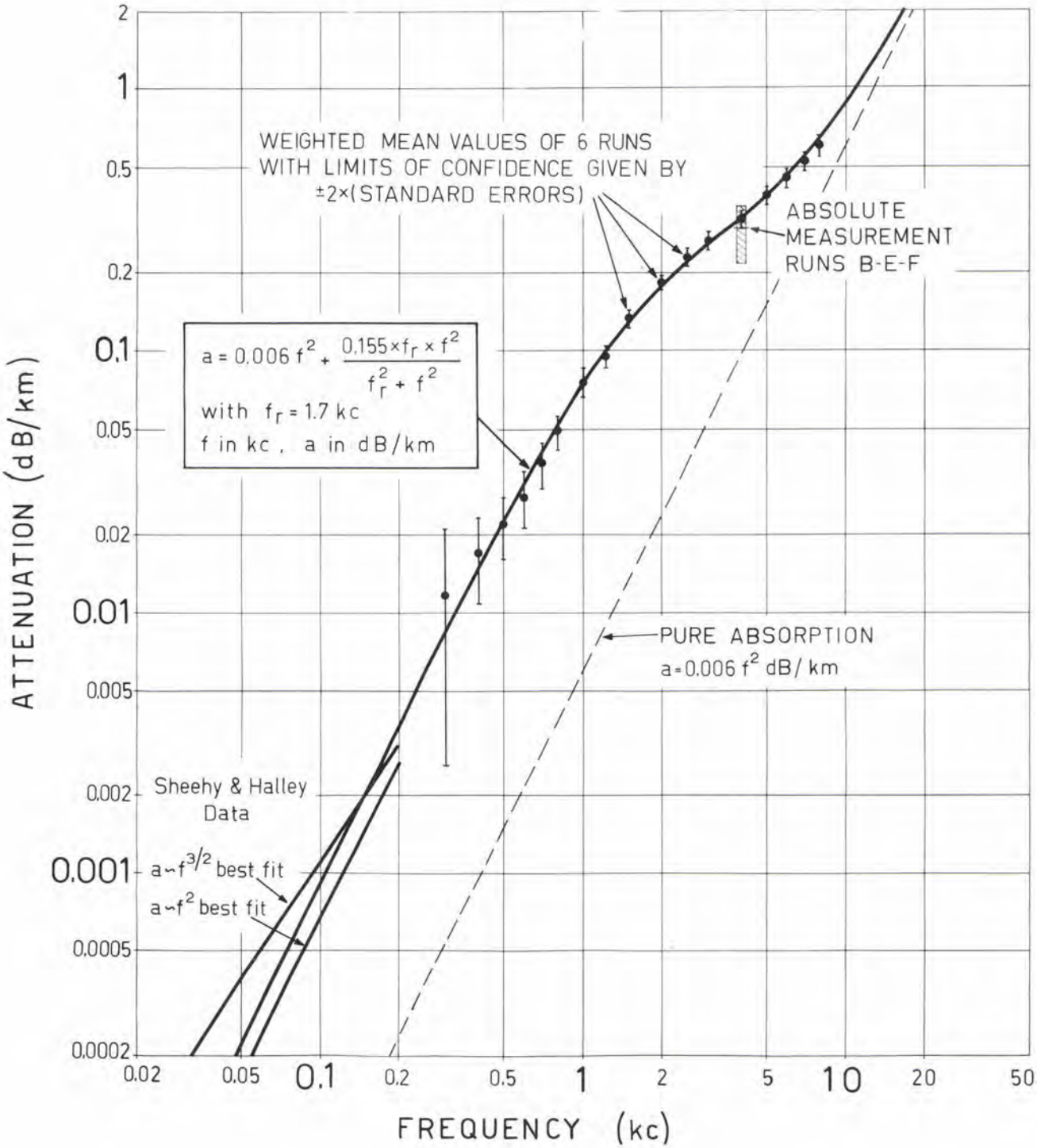

Fig. 10 - SOUND ATTENUATION vs FREQUENCY — FINAL EXPERIMENTAL RESULTS.

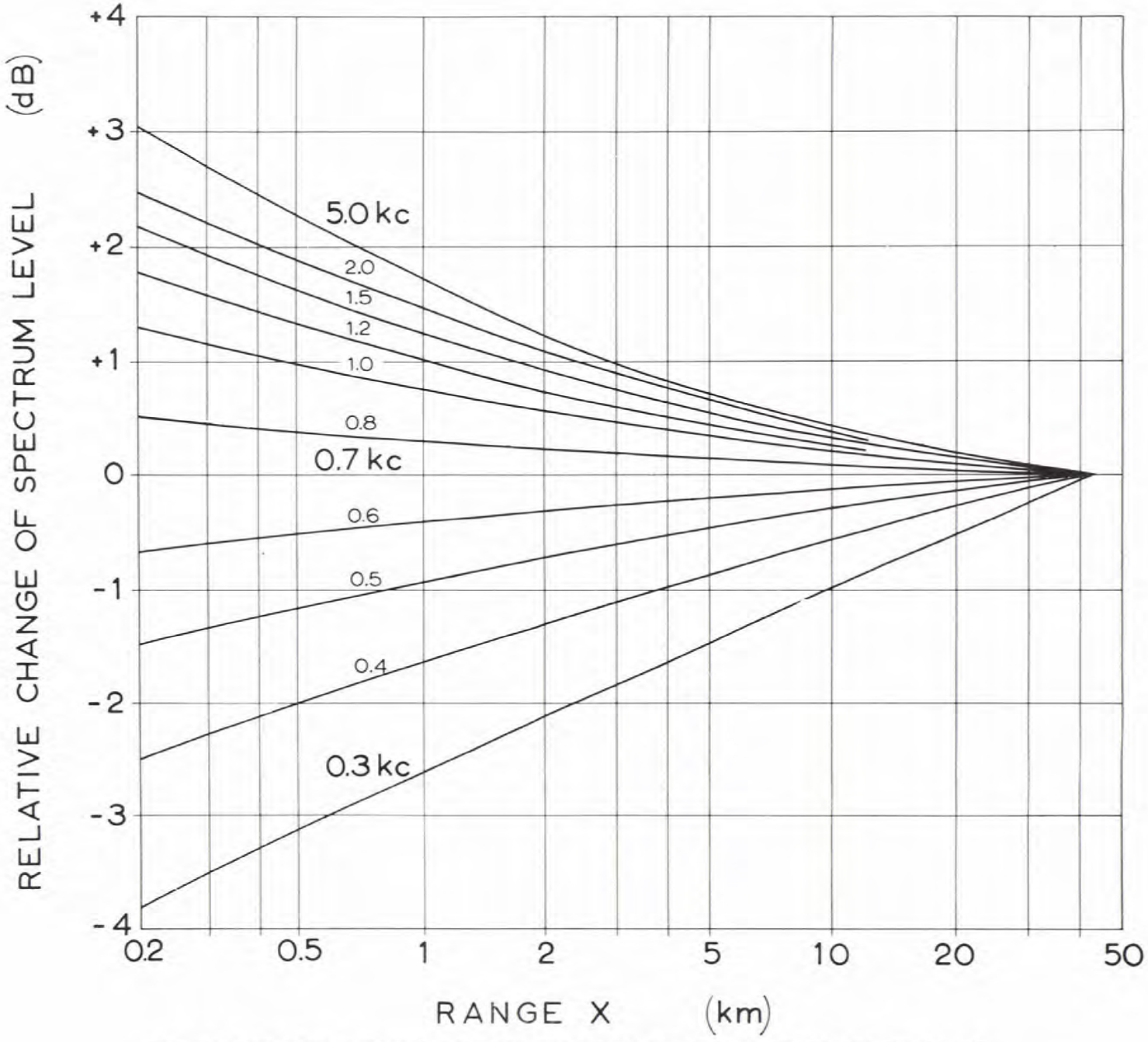

Fig. 11 - RELATIVE CHANGE IN SPECTRUM LEVEL FROM 42 km TO RANGE X DUE TO FINITE AMPLITUDE EFFECTS — ACCORDING TO CLASSICAL THEORY.

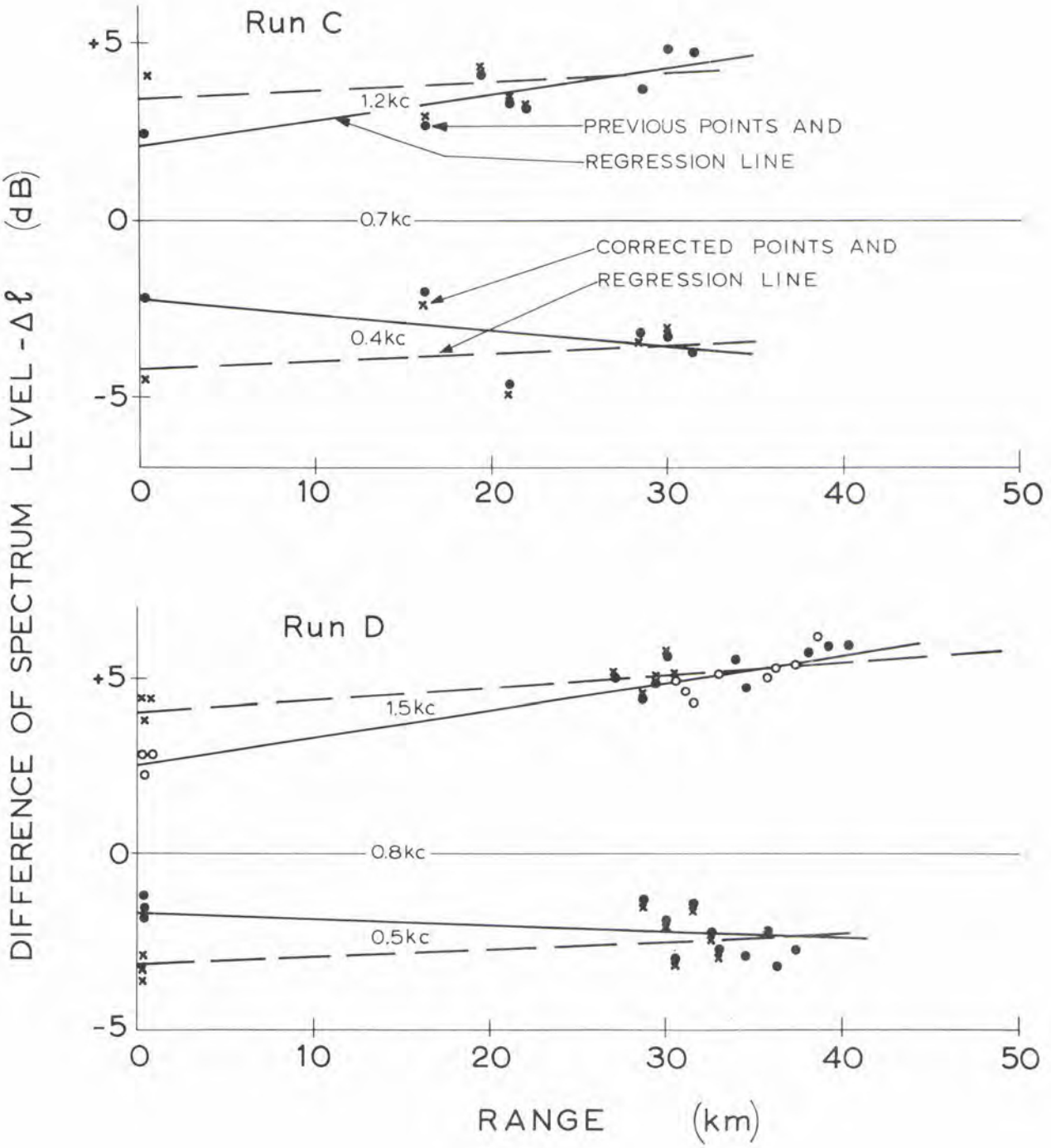

Fig. 12 - EXAMPLES OF REGRESSION ANALYSES OF DATA WITH AND WITHOUT THE CORRECTIONS FOR FINITE AMPLITUDE EFFECTS.

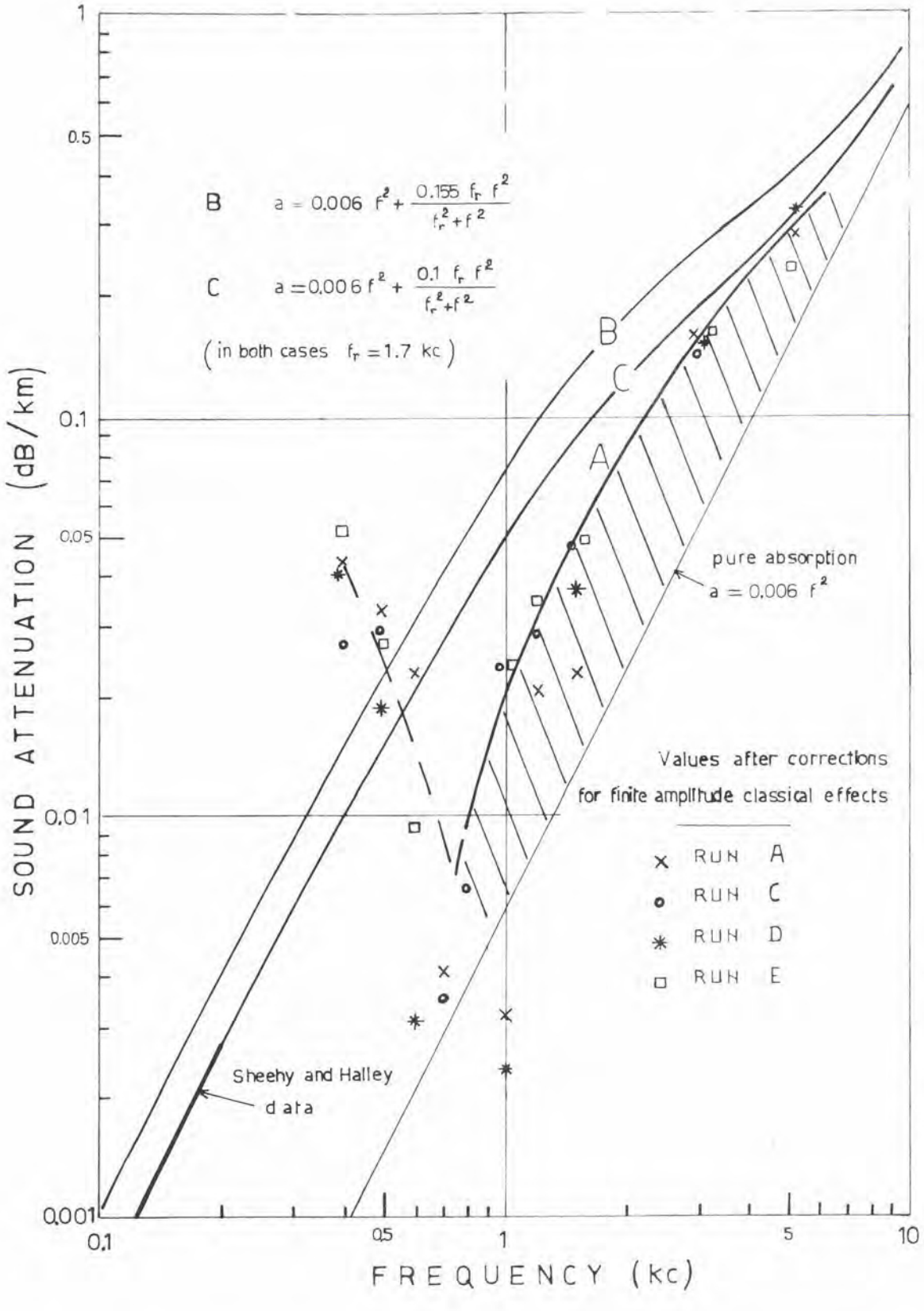

Fig. 13 - SOUND ATTENUATION vs FREQUENCY — MODIFICATION OF EXPERIMENTAL RESULTS BY THE INTRODUCTION OF FINITE AMPLITUDE EFFECTS.

TABLE I

LIST OF THE LINEAR REGRESSIONS PERFORMED, WITH THE NUMBER OF DATA POINTS EMPLOYED IN EACH CASE

Run	Filter	Frequency (kc)															
		0.3	0.4	0.5	0.6	0.7	0.8	1.0	1.2	1.5	2.0	2.5	3.0	4.0	5.0	6.0	7.0	8.0
	I	6	6	6	6	Ref	6	6	6	6	6	--	--	--	--	--	--	--
A	I	--	--	--	6	--	6	6	6	Ref	6	6	6	6	6	--	--	--
	II	--	--	--	--	--	--	--	--	--	--	--	7	7	Ref	7	7	7
	I	--	4	7	7	Ref	7	7	7	7	7	--	--	--	--	--	--	--
B	I	--	--	--	7	--	7	7	7	Ref	7	7	7	7	7	--	--	--
	II	--	--	--	--	--	--	--	--	--	--	--	7	7	Ref	7	7	6
	I	4a	6a	7a	8a	Ref	8a	8a	8a	8a	8a	--	8a	--	--	--	--	--
C	I	--	--	--	8a	--	9a	9a	9a	Ref	9a	9a	9a	9a	9a	--	--	--
	II	--	--	--	--	--	--	--	--	--	--	--	9	9	Ref	8	8	7
	I	11b	11a	Ref	13a	13a	13b	13b	--	--	--	--	--	--	--	--	--	--
	I	11a	11b	--	13a	13a	Ref	13b	--	--	--	--	--	--	--	--	--	--
	II	--	--	--	17	--	Ref	20	20	20	18	--	15	--	--	--	--	--
D	II	--	--	--	17	--	--	20	21	Ref	21	21	18	--	--	--	--	--
	III	--	--	--	--	--	--	--	--	--	--	12	Ref	12	12	12	--	--
	III	--	--	--	--	--	--	--	--	--	--	12	--	--	Ref	12	12	9
E	I	8	10	13	13	Ref	13	13	13	13	13	--	--	--	--	--	--	--
	I	--	--	--	13	--	13	13	13	Ref	13	13	13	12	11	--	--	--
F	I	7a	7	8	8	Ref	8	8	8	8	8	--	--	--	--	--	--	--
	I	--	--	--	8	--	10	10	10	Ref	10	10	10	10	9	--	--	--

For runs A, B and C, Filter I = wide band (150–8000 cps). Filter II = 2500–10000 cps. For run D Filter I = 280–1050 cps, Filter II = 240–3700 cps, Filter III = 2400–9600 cps. For runs D and F Filter I = wide band (70–6000 cps).

All the non-indexed numbers correspond to data points which were weighted in the regression. An index 'a' means that data were not weighted. An index 'b' means that both weighted and unweighted regressions were performed. In addition, the following regressions were performed for run D; Filter I; 0.9/0.5 Kc with 13 unweighted points. Filter II; 3.5/1.5 Kc with 17 points. Filter III; 3.5/3 Kc and 3.5/5 Kc with 12 points

TABLE II

DIFFERENTIAL ATTENUATION COEFFICIENTS Δa IN dB/Km x 10^{-3}, WITH THEIR STANDARD ERROR S.E. IN THE SAME UNITS

(a) Coefficients Calculated with Respect to f_o = 0.7 Kc from the Wide Band Oscillograms of Runs A, B, C, E, F.

Frequency (kc)	Run A		Run B		Run C		Run E		Run F	
	Δa	S.E.	Δa	S.E.	Δa	S.E.	Δa	S.E.	Δa	S.E.
0.3	−16.9	6.9	--	--	−34.5	24.7	−10.5	16.5	−6.3	10.0
0.4	−12.0	6.0	−54	10	−42.8	34.1	−12.4	7.1	−10.4	6.5
0.5	−8.3	3.3	−47.8	14.2	−35.1	23.4	−10.0	2.6	−14.7	4.0
0.6	−4.3	2.1	−23.5	8.4	−22.0	11.7	−7.9	8.3	−11.5	2.2
0.7	0	--	0	--	0	--	0	--	0	--
0.8	8.9	2.8	25.0	3.6	18.9	7.2	12.5	4.3	17.4	3.0
1.0	30.9	4.2	55	3	52.3	15.7	49.6	12.6	58	11
1.2	57	4	75	12	73	22	72	19	89	15
1.5	96	5	101	16	107	22	100	15	131	14
2.0	156	4	132	26	142	37	144	27	201	18

(b) Coefficients Calculated at Low Frequencies from Run D (1st and 2nd Series of Filtered Oscillograms)

Frequency (kc)	Analysis from filter I (280–1050 cps)				Analysis from filter II (240–3700 cps)		
	Δa	S.E.	Δa	S.E.	Δa	S.E.	
0.3	−15.5	6.4a	−41.3	11.4	--	--	
0.4	6.3	3.6	−36.0a	10.0a	--	--	
0.5	0	--	−29.9	11.3	--	--	
0.6	7.1	5.2	−22.8	7.9	−25.8	5.4	a. Average of Linear Regressions with Unweighted and Weighted Data.
0.7	18.2	9.3	−11.7	3.4	--	--	
0.8	30.2a	8.9a	0	--	0	--	
0.9	42.6	10.9	--	--	--	--	
1.0	55.2a	8.6a	24.9a	5.5a	20.5	4.0	
1.2	--	--	--	--	35.5	4.9	
1.5	--	--	--	--	78.0	5.1	
2.0	--	--	--	--	130	8	
3.0	--	--	--	--	196	11	

TABLE II (Continued)

(c) Coefficients Calculated with Respect to 1.5 Kc, from the 6 Runs (from Wide Band Oscillograms for A, B, C, E, F. From Filtered Oscillograms (240–3700 cps) for D)

Frequency (kc)	Run A		Run B		Run C		Run D		Run E		Run F	
	Δa	S.E.	Δa	S.E.	Δa	S.E.	Δa	S.E.	Δa	S.E.	Δa	S.E.
0.6	−107	5	−125	20	−129	28	−102	9	−108	18	−142	18
0.7	−96	5	−101	16	−107	22	--	--	−100	15	−131	14
0.8	−87	3	−76	15	−87	17	−78.0	5.1	−89	14	−111	13
1.0	−65	6	−46.2	15.2	−55.8	8.9	−57.5	4.2	−56	10	−71	8
1.2	−39.4	2.4	−24.9	9.3	−33.9	3.4	−42.1	5.2	−28.4	7.1	−42	5
1.5	0	--	0	--	0	--	0	--	0	--	0	--
2.0	60	6	31.3	10.8	39.4	32.1	50.1	3.8	44.9	13.7	64	10
2.5	104	14	76	18	84	29	94	10	66	29	80	30
3.0	141	19	104	19	106	30	122	10	117	37	136	30
3.5	--	--	--	--	--	--	159	12	--	--	--	--
4.0	217	27	158	16	184	44	--	--	153	86	160	22
5.0	273	36	242	30	246	75	--	--	201	90	230	81

(d) Coefficients Calculated at the Higher Frequencies from the Filtered Oscillograms of Runs A, B, C (2500–10000 cps) and D (2400–9600 cps)

Frequency (kc)	Run A		Run B		Run C		Run D			
	Δa	S.E.	Δa	S.E.	Δa	S.E.	Δa	S.E.	Δa	S.E.
2.5	--	--	--	--	--	--	−179	32	−20.2	6.4
3.0	−107	16	−96	20	−158	36	−158	32	0	--
3.5	--	--	--	--	--	--	−137	29	20.8	5.5
4.0	−42.3	9.4	−45.7	10.8	−81	23	--	--	45.3	15.4
5.0	0	--	0	--	0	--	0	--	158	32
6.0	47.5	8.9	55.3	14.3	75	10	63	11	218	40
7.0	121	20	128	30	153	17	110	15	--	--
8.0	211	43	197	36	234	59	164	51	--	--

TABLE III

DIFFERENCES OF SPECTRUM LEVELS $\Delta \ell$, IN dB, MEASURED IN RUN C

	Frequency (kc)	Range X (Km) 0.3	2.1	16.2	19.4	21.0	22.0	28.5	30.0	31.5
(a) $\Delta \ell$ measured from the wide band oscillograms spectra with respect to f_o = 0.7 Kc	0.3	3.4	--	3.0	--	--	--	4.5	4.1	--
	0.4	2.4	--	2.1	--	4.7	--	3.3	3.2	3.7
	0.5	1.4	--	1.3	2.6	3.2	--	2.1	2.3	2.6
	0.6	0.6	--	0.6	1.2	1.6	0.8	1.0	1.3	1.3
	0.8	-0.6	--	-0.6	-1.0	-1.1	-0.7	-0.9	-1.1	-1.3
	1.0	-1.6	--	-1.7	-2.6	-2.5	-2.0	-2.4	-3.3	-3.3
	1.2	-2.4	--	-2.7	-4.1	-3.3	-3.1	-3.6	-4.9	-4.7
	1.5	-3.4	--	-4.2	-5.6	-4.7	-4.8	-5.6	-6.9	-6.7
	2.0	-4.8	--	-6.1	-7.7	-7.4	-9.8	-8.0	-9.5	-8.8
	3.0	-7.1	--	-10.5	-11.1	-9.7	-13.0	-12.8	-14.0	-13.2
(b) $\Delta \ell$ measured from the wide band oscillogram spectra with respect to f_o = 1.5 Kc	0.6	4.0	--	4.8	6.8	6.3	5.6	6.6	8.2	8.0
	0.7	3.4	--	4.2	5.6	4.7	4.8	5.6	6.9	6.7
	0.8	2.8	2.7	3.6	5.0	3.6	4.1	4.7	5.8	5.4
	1.0	1.8	1.7	2.5	3.0	2.2	2.8	3.2	3.6	3.4
	1.2	1.0	1.0	1.5	1.5	1.4	1.7	2.0	2.0	2.0
	2.0	-1.4	-1.6	-1.9	-2.1	-2.7	-5.0	-2.4	-2.6	-2.1
	2.5	-2.6	-2.8	-4.0	-4.0	-3.8	-6.6	-5.8	-4.8	-4.5
	3.0	-3.7	-4.1	-6.3	-5.5	-5.0	-8.2	-7.2	-7.1	-6.5
	4.0	-6.1	-6.1	-8.6	-11.5	-7.8	-12.2	-10.6	-11.9	-11.3
	5.0	-8.6	-7.6	-12.9	-18.1	-11.8	-16.9	-13.9	-15.2	-15.7
(c) $\Delta \ell$ measured from the filtered oscillogram spectra with respect to f_o = 5 Kc	3.0	2.7a	2.5/3.0	7.5a	9.0	3.9	8.1	5.6a	7.6a	8.6a
	4.0	1.5a	1.5/1.8	3.9a	6.0	2.4	4.3	2.9a	4.1a	4.6a
	6.0	-1.8a	-2.2/2.3	-3.5a	--	-2.6	-4.1	-3.5a	-4.4a	-4.6a
	7.0	-3.4a	-5.2/5.0	-7.1a	--	-5.6	-7.6	-8.1a	-9.1	-9.1a
	8.0	-5.9	-8.0/8.2	-10.6a	--	-8.3	--	-15.2	-14.9	-13.2

TABLE IV

DIFFERENTIAL COEFFICIENTS OF ATTENUATION Δa, WITH THEIR STANDARD ERRORS S.E., IN dB/Km x 10^{-3} CALCULATED FROM THE BUBBLE PULSE ANALYSIS OF RUN C, SHOWING THE COMPARISON WITH OTHER RESULTS

Frequency (kc)	Values Calculated from Run C			Values given by pure Absorption
	Bubble Pulse Analysis		Shock Wave Analysis	
	Δa	S.E.	Δa	Δa
1.5	-91	35	-106	-40.5
2.0	-112	42	-77	-30
2.5	-75	18	-22	-16.5
3.0	0	--	0	0
3.5	53	14	--	19.5
4.0	90	37	78	42

TABLE V

DIFFERENTIAL COEFFICIENTS OF ATTENUATION Δa, WITH THEIR STANDARD ERRORS S.E., IN dB/Km x 10^{-3}, CALCULATED FROM RUN G, SHOWING THE COMPARISON WITH OTHER RESULTS

Frequency (kc)	Values Obtained from Run G				Average Values from Runs A to F	Values Given by pure Absorption
	Shock Wave Analysis		Bubble Pulse Analysis			
	Δa	S.E.	Δa	S.E	Δa	Δa
0.8	-60	19	-80	38	-85	-9.8
1.0	-39.6	19.5	-47.9	33.2	-59	-6.0
1.2	--	--	-27.2	19.8	-37.5	-4.9
1.5	0	--	0	--	0	0
2.0	--	--	59	26	52.2	10.5
2.5	53	82	87	39	91	24.0
3.0	110	37	110	53	122	40.5
3.5	167	44	146	54	--	60
4.0	251	52	205	80	170	82

TABLE VI

DIFFERENTIAL COEFFICIENTS OF ATTENUATION Δa, WITH THEIR STANDARD ERRORS S.E. IN dB/Km x 10^{-3}, RESULTING FROM ANALYSES WHERE THE DATA POINTS HAVE BEEN CORRECTED FOR FINITE AMPLITUDE EFFECTS ACCORDING TO THE CLASSICAL THEORY

	Frequency (kc)	Run A		Run C		Run D				Run E	
						From Filter I		From Filter II			
		Δa	S.E.	Δa	S.E.	Δa	S.E.	Δa	S.E.	Δa	S.E.
Differential values in the low frequency region	0.4	39.2	2.2	23	37	21.9	3.8	--	---	51.1	6.4
	0.5	28.3	1.7	25	22	0	--	--	--	26.0	10.6
	0.6	18.3	1.7	-3.4	12.1	-16.3	5.5	--	--	8.3	7.3
	0.7	0	--	0	--	-19.3	9.9	0	--	0	--
	0.8	-4.0	2.1	3.1	8.3	-18.8	12.4	1.8	4.7	-0.8	3.5
	1.0	-0.9	2.2	19.8	19.5	--	--	--	--	24.0	12.3
	1.2	16.4	3.6	24.6	27.1	--	--	36.1	5.8	34.9	10.8
	1.5	18.4	14.3	44	76	--	--	--	--	52.4	15.4
Differential value between 1.5 and 3.0 Kc		125	20	90	29	105	10	--	--	104	36
Differential value between 3.0 and 5.0 Kc		118	32	--	--	156	31	--	--	68	55

DISTRIBUTION LIST

Minister of Defense Brussels, Belgium	10 copies
Minister of National Defense Department of National Defense Ottawa, Canada	10 copies
Chief of Defense, Denmark Kastellet Copenhagen Ø, Denmark	10 copies
Minister of National Defense Division Transmissione-Ecoute-Radar 51 Latour Maubourg Paris 7e, France	10 copies
Minister of Defense Federal Republic of Germany Bonn, Germany	10 copies
Minister of Defense Athens, Greece	10 copies
Ministero della Difesa Stato Maggiore Marina Roma, Italy	10 copies
Minister of National Defense Plein 4, The Hague, Netherlands	10 copies
Minister of National Defense Storgaten 33, Oslo, Norway	10 copies
Minister of National Defense Lisboa, Portugal	10 copies
Minister of National Defense Ankara, Turkey	10 copies
Minister of Defense London, England	20 copies
Supreme Allied Commander Atlantic (SACLANT) Norfolk 23511, Virginia	3 copies
SACLANT Representative in Europe (SACLANTREPEUR) Place du Marechal de Lattre de Tassigny Paris 16e, France	1 copy
Commander in Chief Western Atlantic Area (CINCWESTLANT) Norfolk 23511, Virginia	1 copy
Commander in Chief Eastern Atlantic Area (CINCEASTLANT) Eastbury Park, Northwood Middlesex, England	1 copy
Maritime Air Commander Eastern Atlantic Area (COMAIREASTLANT) R.A.F. Northwood Middlesex, England	1 copy
Commander Submarine Force Eastern Atlantic (COMSUBEASTLANT) Fort Blockhouse Gosport, Hants, England	1 copy
Commander, Canadian Atlantic (COMCANLANT) H.M.C. Dockyard Halifax, Nova Scotia	1 copy
Commander Ocean Sub-Area (COMOCEANLANT) Norfolk 23511, Virginia	1 copy
Supreme Allied Commander Europe (SACEUR) Paris, France	7 copies
SHAPE Technical Center P.O. Box 174 Stadhouders Plantsoen 15 The Hague, Netherlands	1 copy
Allied Commander in Chief Channel (CINCCHAN) Fort Southwick, Fareham Hampshire, England	1 copy
Commander Allied Maritime Air Force Channel (COMAIRCHAN) Northwood, England	1 copy
Commander in Chief Allied Forces Mediterranean (CINCAFMED) Malta, G.C.	1 copy
Commander South East Mediterranean (COMEDSOUEAST) Malta, G.C.	1 copy

Commander Central Mediterranean
(COMEDCENT)
Naples, Italy — 1 copy

Commander Submarine Allied
Command Atlantic
(COMSUBACLANT)
Norfolk 23511, Virginia — 1 copy

Commander Submarine Mediterranean
(COMSUBMED)
Malta, G.C. — 1 copy

Standing Group, NATO
(SGN)
Room 2C256, The Pentagon
Washington 25, D.C. — 3 copies

Standing Group Representative
(SGREP)
Place du Marechal de Lattre de Tassigny
Paris 16^{e}, France — 5 copies

ASG for Scientific Affairs
NATO
Porte Dauphine
Paris 16e, France — 1 copy

National Liaison Representatives

NLR Belgium
Belgian Military Mission
3330 Garfield Street, N.W.
Washington, D.C. — 1 copy

NLR Canada
Canadian Joint Staff
2450 Massachusetts Avenue, N.W.
Washington, D.C. — 1 copy

NLR Denmark
Danish Military Mission
3200 Massachusetts Avenue, N.W.
Washington, D.C. — 1 copy

NLR France
French Military Mission
1759 "R" Street, N.W.
Washington, D.C. — 1 copy

NLR Germany
German Military Mission
3215 Cathedral Avenue, N.W.
Washington, D.C. — 1 copy

NLR Greece
Greek Military Mission
2228 Massachusetts Avenue, N.W
Washington, D.C. — 1 copy

NLR Italy
Italian Military Mission
3221 Garfield Street, N.W.
Washington, D.C. — 1 copy

NLR Netherlands
Netherlands Joint Staff Mission
4200 Linneau Avenue
Washington, D.C. 20008 — 1 copy

NLR Norway
Norwegian Military Mission
2720 34th Street, N.W.
Washington, D.C. — 1 copy

NLR Portugal
Portuguese Military Mission
2310 Tracy Place, N.W
Washington, D.C. — 1 copy

NLR Turkey
Turkish Joint Staff Mission
2125 LeRoy Place, N.W.
Washington, D.C. — 1 copy

NLR United Kingdom
British Defence Staffs, Washington
3100 Massachusetts Avenue, N.W.
Washington, D.C. — 1 copy

NLR United States
SACLANT
Norfolk 23511, Virginia — 40 copies

Scientific Committee of National Representatives

Dr. W. Petrie
Defence Research Board
Department of National Defence
Ottawa, Canada — 1 copy

G. Meunier
Ingenieur en Chef des Genie Maritime
Services Technique des Constructions et Armes Navales
8 Boulevard Victor
Paris 15^{e}, France — 1 copy

Dr. E. Schulze
Bundesministerium der Verteidigung
ABT H ROMAN 2/3
Bonn, Germany — 1 copy

Commander A. Pettas
Ministry of National Defense
Athens, Greece — 1 copy

Professor Dr. M. Federici
Segreteria NATO
MARIPERMAN
La Spezia — 1 copy

Dr. M.W. Van Batenburg
Physisch Laboratorium RVO-TNO
Waalsdorpvlakte
The Hague, Netherlands — 1 copy

Mr. A.W. Ross
Director of Naval Physical Research
Ministry of Defence (Naval)
Bank Block
Old Admiralty Building
Whitehall, London S.W. 1 — 1 copy

Dr. J.E. Henderson
Applied Physics Laboratory
University of Washington
1013 Northeast 40th Street
Seattle 5, Washington — 1 copy

Capitaine de Fregate R.C. Lambert
Etat Major Général Force Navale
Caserne Prince Baudouin
Place Dailly
Bruxelles, Belgique — 1 copy

CAPT H. L. Prause
Sóvaernets Televaesen
Lergravsvej 55
Copenhagen S', Denmark — 1 copy

Mr. F. Lied
Norwegian Defense Research
Establishment
Kjeller, Norway — 1 copy

Ing. CAPT N. Berkay
Seyir Ve HDR D
CUBUKLU
Istanbul, Turkey — 1 copy

National Liaison Officers

Mr. Sv. F. Larsen
Danish Defense Research Board
Østerbrogades Kaserne
Copenhagen Ø, Denmark — 1 copy

CDR R. J. M. Sabatier
EMM/TER
2 Rue Royale
Paris 8e, France — 1 copy

Capitano di Fregata U. Gilli
Stato Maggiore della Marina
Roma, Italia — 1 copy

LCDR J.W. Davis, USN
Office of Naval Research
Branch Office, London
Box 39, Fleet Post Office
New York, N.Y. 09510 — 1 copy

CDR Jose E.E.C. de Ataide
Instituto Hydrografico
Rua Do Arsenal Porta H-1
Lisboa 2, Portugal — 1 copy